NIST Special Publication 1039r1

# Liquid Flow Meter Calibrations with the 0.1 L/s and the 2.5 L/s Piston Provers

Jodie G. Pope
John D. Wright
Aaron N. Johnson
Chris J. Crowley

http://dx.doi.org/10.6028/NIST.SP.1039r1

National Institute of Standards and Technology
U.S. Department of Commerce

**NIST Special Publication 1039r1**

# Liquid Flow Meter Calibrations with the 0.1 L/s and the 2.5 L/s Piston Provers

Jodie G. Pope
John D. Wright
Aaron N. Johnson
Chris J. Crowley
*Office of Sensor Science Division*
*Physical Measurement Laboratory*

http://dx.doi.org/10.6028/NIST.SP.1039r1

April 2014

U.S. Department of Commerce
*Penny Pritzker, Secretary*

National Institute of Standards and Technology
*Patrick D. Gallagher, Under Secretary of Commerce for Standards and Technology and Director*

**National Institute of Standards and Technology Special Publication 1039r1**
**Natl. Inst. Stand. Technol. Spec. Publ. 1039r1, 53 pages (September and 2013)**
**http://dx.doi.org/10.6028/NIST.SP.1039r1**
**CODEN: NSPUE2**

# LIQUID FLOW METER CALIBRATIONS WITH THE 0.1 L/S AND 2.5 L/S PISTON PROVERS

NIST Special Publication 250-1039r1

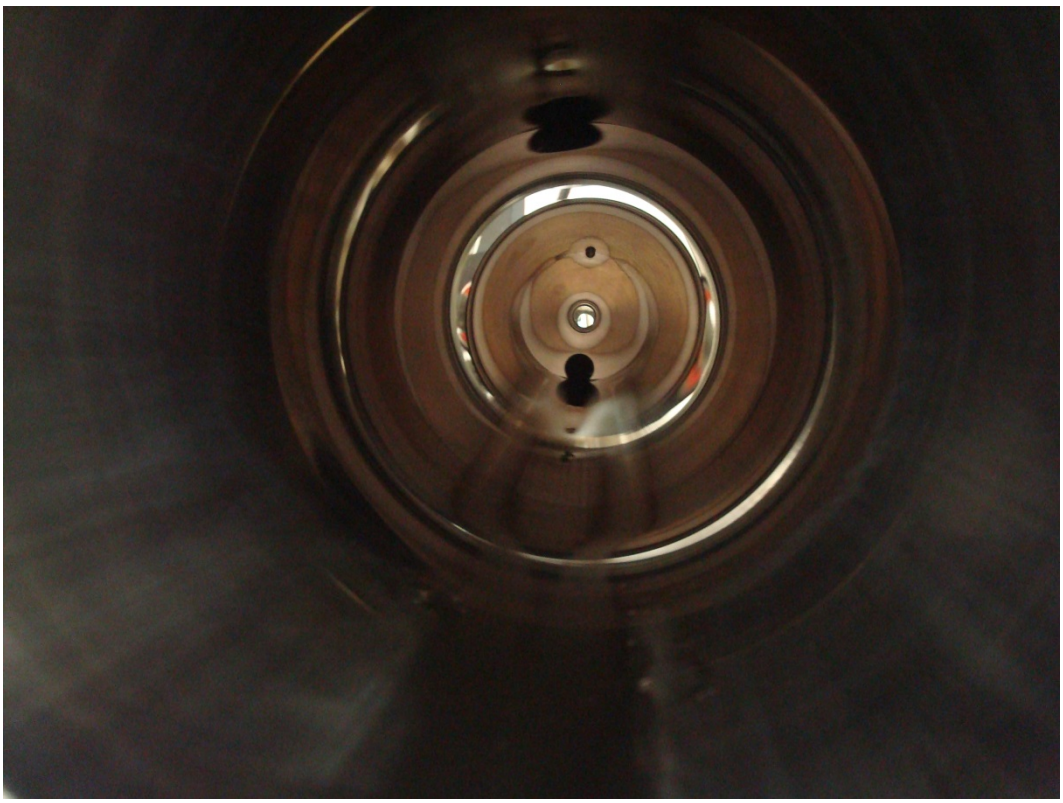

Jodie G. Pope, John D. Wright, Aaron N. Johnson, and Chris J. Crowley

April 17, 2014

Fluid Metrology Group
Sensor Science Division
Physical Measurement Laboratory
National Institute of Standards and Technology
Gaithersburg, MD 20899-8361

**Liquid Flow Meter Calibrations with the 0.1 L/s and 2.5 L/s Piston Provers**

**Table of Contents**

**Abstract**

This document provides a description of the 2.5 L/s and 0.1 L/s liquid flow calibration standards operated by the National Institute of Standards and Technology (NIST) Fluid Metrology Group to provide flow meter calibrations for customers. The 0.1 L/s and 2.5 L/s flow standards measure flow by moving a piston of known cross-sectional area over a measured length during a measured time. The 0.1 L/s standard uses a passive piston prover technique where fluid is driven by a pump that in turn moves the piston. The 2.5 L/s standard uses a variable speed motor and drive screw to move the piston and thereby move the fluid through the system. The fluid medium used in these standards is a propylene glycol and water mixture that has kinematic viscosity of approximately 1.2 cSt at 21 °C (1 cSt = 1 x $10^{-6}$ $m^2/s$), but the ratio of propylene glycol to water can be altered to offer a range of fluid properties. The 0.1 L/s standard has an expanded uncertainty of ± 0.044 %, spanning the flow range 0.003 L/s to 0.1 L/s (0.05 gal/min to 1.5 gal/min). The 2.5 L/s standard has an expanded uncertainty of ± 0.064 %, spanning the flow range 0.02 L/s to 2.0 L/s (0.3 gal/min to 31 gal/min) (Here, expanded uncertainties correspond to a 95 % confidence level).

This document provides an overview of the liquid flow calibration service and the procedures for customers to submit their flow meters to NIST for calibration. We derive the equation for calculating flow at the meter under test, including the corrections for storage effects caused by changes in fluid density in the connecting volume (due to temperature changes). Finally, we analyze the uncertainty of the flow standards, give supporting data, and provide a sample calibration report.

Key words: calibration, flow, connecting volume, flow meter, flow standard, uncertainty

## 1.0 Introduction

Flow measurement units are derived from the SI base units. Therefore, the paths taken to realize flow measurement standards vary and depend upon such issues as the properties of the fluid(s) to be measured. Realization methods at NIST are always derived from fundamental measurements such as mass, length, time, and temperature, typically by accounting for the transfer of a known mass or volume of fluid during a measured time interval under approximately steady state conditions of flow, pressure, and temperature at the meter under test (MUT). Such flow metrology facilities are known as "primary flow standards", and by definition [1], they are facilities capable of determining flow, at specific, quantifiable uncertainty levels, while being traceable to more fundamental units of measure (e.g. length, time, *etc*.), and not calibrated against another flow device. This document describes a 0.1 L/s Liquid Flow Standard (LFS) that covers flows up to

0.1 L/s with expanded uncertainty of 0.044 % and a 2.5 L/s LFS that covers flows up to 2.5 L/s with expanded uncertainty of 0.064 % (with a 95 % confidence level)[a].

The 0.1 L/s and 2.5 L/s LFSs each consist of a fluid source (e.g., tank), a long, straight test section that provides a fully-developed flow profile, stable temperature and pressure, and a system for timing the displacement of a quantity of the fluid. The flow measured by the primary standard is computed along with the average of the flow indicated by the MUT during the collection interval. All of the quantities measured in connection with the calibration standards (i.e., temperature, pressure, density, time, etc.) are traceable to established national standards.

NIST calibrates liquid flow meters to provide traceability for flow meter manufacturers, secondary flow calibration laboratories, and flow meter users. We calibrate a customer's flow meter and deliver a calibration report that documents the calibration procedure, the calibration results, and their uncertainty on a fee-for-service basis. The customer may use the flow meter and its calibration results in different ways. The flow meter is often used as a transfer standard to compare the customer's primary standards to the NIST primary standards so that the customer can establish traceability, validate their uncertainty analysis, and demonstrate proficiency. Customers with no primary standards use their NIST-calibrated flow meters as working standards or reference standards in their laboratory to calibrate other flow meters. The Report of Calibration is the property of the customer and NIST treats the results of calibrations as proprietary information belonging to the customer.

Operators of primary flow standards seek to validate the claimed uncertainties of their standards by establishing and maintaining the traceability of calibration results to the SI. One complete way to establish traceability involves the use of proficiency testing techniques, which quantify the traceability of a facility's results using a set of flow standards maintained by a National Metrology Institute (NMI) [2]. Alternatively, establishing traceability can be achieved through assessment of individual facility components and analyzing their respective contributions to the calibration process. A detailed uncertainty analysis of NIST's LFSs is described in following sections of this document using the component analysis method [3].

## 2.0 Description of Measurement Services

Customers should consult the web address http://www.nist.gov/calibrations/flow_measurements.cfm#18020C to find the most current information regarding NIST's calibration services, calibration fees, technical contacts, and flow meter submittal procedures.

---

a Standard uncertainty with coverage factor $k = 1$, refers to 65 % confidence level and expanded uncertainty with $k = 2$ refers to 95 % confidence level. For expanded uncertainty $k \approx 2$; however, effective degrees of freedom and the associated $t$-value must be considered for the true $k$ value corresponding to 95 % confidence level.

NIST uses the LFSs described herein to provide liquid flow meter calibrations for flows between 0.003 L/s and 2.5 L/s [4]. The most common flow meter types received for calibrations are turbines, Coriolis meters, and positive displacement (PD) meters. NIST's LFSs are designed to acquire square-wave pulse outputs from the MUT. The liquid used for calibrations is normally a 5 % by volume propylene glycol and water mixture (PGW). The facility can be used with varying PGW mixtures with varying physical properties, but this is a Special Test and should be discussed with the technical contacts before a flow meter is submitted for such a calibration. The liquid temperature during the calibration is 22 ± 1 °C. NIST has a supply of fittings designated Swagelok[b], A/N 37 degree flare, and national pipe thread (NPT) for installing flow meters into the LFSs for calibration.

Meters are tested if the flow range and piping connections are suitable and have precision appropriate for calibration with the NIST flow measurement uncertainty. Meter types with calibration instability significantly larger than the primary standard uncertainty are generally not calibrated with the NIST standards because such meters can be calibrated with acceptable uncertainties at a lower cost by commercial labs.

A normal flow calibration performed by NIST's Fluid Metrology Group consists of five flows spanning the range of the flow meter. A flow meter is normally calibrated at 10 %, 30 %, 50 %, 75 %, and 100 % of its full scale. At each of these flow set points, five flow measurements are made consecutively. The same set point flows are tested on a second occasion. Therefore, the final data set consists of ten flow measurements made at five flow set points, i.e., 50 individual flow measurements. The sets of five measurements can be used to assess repeatability, while the sets of ten can be used to assess reproducibility [1]. For an example, see the sample calibration report in Appendix A of this document. Variations on the number of flow set points, spacing of the set points, and the number of repeated measurements can be discussed with the NIST technical contacts. However, for data quality assurance reasons, NIST rarely conducts calibrations involving fewer than three flow set points and two sets of three flow measurements at each set point.

The Fluid Metrology Group prefers to present flow meter calibration results in a dimensionless format that takes into account the physical model for the flow meter type. The dimensionless approach facilitates accurate flow measurements by the flow meter user even when the conditions of usage (liquid type, temperature) differ from the conditions during calibration. Hence for a turbine meter calibration, the calibration report will present Strouhal number vs. Roshko number [5, 6]. In order to calculate the uncertainty of these flow meter calibration factors, we must know the uncertainty of the standard flow measurement as well as the uncertainty of the instrumentation associated with the MUT (normally

b Certain commercial equipment, instruments, or materials are identified in this paper to foster understanding. Such identification does not imply recommendation or endorsement by the National Institute of Standards and Technology, nor does it imply that the materials or equipment identified are necessarily the best available for the purpose.

frequency and temperature instrumentation). NIST-owned and controlled instruments (temperature, etc.) are used as part of the test of a customer's meter since these have established uncertainty values based on calibration records maintained as part of NIST's Quality System: http://www.nist.gov/qualitysystem/index.cfm. Such information is not available for the customer's instrumentation. Use of the customer's instrumentation for a calibration or Special Test requires specific arrangements with the NIST technical contact. Calibration of customer's ancillary instrumentation is not part of the calibration procedures described here and would require that separate arrangements be made.

Following calibration, meters are rinsed with ethanol and dried. This precaution avoids contaminating customers' fluids with water that remains in the meter and it prevents corrosion of any part of the meter that is incompatible with water. Most meters can be simply rinsed with alcohol using a hand held squirt bottle, or capped, filled with alcohol, inverted several times to fill and mix trapped volumes, and drained. Some meters (*e.g.* positive displacement meters) may have crevices that retain water if not rinsed more aggressively. NIST rinses such meters in a recirculating flow of ethanol at approximately 15 % of the maximum flow for a minimum of five minutes. During the rinse, the meter is installed so that the RF or magnetic pickoff of the positive displacement meter is positioned downward. This precaution assures that all water is removed from the relatively small cavity enclosing the pickup if the meter has such a cavity. There are multiple acceptable ways to dry flow meters: 1) application of vacuum, 2) application of a stream of dry gas, and 3) by hanging and waiting for draining and evaporation. For turbine and positive displacement meters, one end of the meter is capped while vacuum is applied to the other for one hour. This method avoids over-spinning the turbine or PD meter that might occur if too strong a stream of dry gas is applied. However, Coriolis meters are dried using a stream of dry nitrogen because it is quicker and over-spinning is not a concern with this meter type. In the event that no vacuum or inert gas is available, meters are hung to dry at various orientations for a minimum of three hours at each orientation to be sure all void volumes in the meter have drained dry.

### 3.0 Procedures for Submitting a Flow meter for Calibration

The Fluid Metrology Group follows the NIST calibrations policies which can be found at the following addresses:
http://www.nist.gov/calibrations/policy.cfm,
http://www.nist.gov/calibrations/domestic.cfm, and
http://www.nist.gov/calibrations/foreign.cfm.
The web site gives instructions for ordering a calibration for domestic and foreign customers and has the sub-headings: A.) Customer Inquiries, B.) Pre-arrangements and Scheduling, C.) Purchase Orders, D.) Shipping, Insurance, and Risk of Loss, and E.) Turnaround Time. The web site also gives special instructions for foreign customers. The web address: http://www.nist.gov/calibrations/mechanical_index.cfm has information more specific to the flow calibration service, including the technical contacts in the Fluid Metrology Group, fee estimates, and turnaround times.

## 4.0 Description of the Liquid Flow Standards

Piston prover systems have long been accepted as primary flow standards for both gas and liquid flow meters [7,8]. Figure 1 shows NIST's piston provers and Table 1 and Table 2 give their characteristics. Conceptually, a piston prover consists of a circular cylinder of known internal diameter surrounding a sealed piston. This piston strokes through measured lengths, at a constant speed, to produce a constant volumetric flow. The volumetric flow is calculated by dividing the swept volume by the time needed for the piston to traverse the measured length. Alternatively, a water draw can be performed to determine the volumetric prover factor, $K_V^{ref}$, which is the number of encoder pulses divided by the volume of fluid pushed through the cylinder. Temperature (and pressure for the 2.5 L/s LFS) measurements at key locations are used to assess the changes in fluid density and connecting volume that occur between the start and stop times, allowing corrections for storage effects. The calibration fluid coefficient of thermal expansion is known, hence the volumetric flow in the cylinder can be converted to the volumetric flow at the test section where the MUT is located (or the mass flow can be calculated using the fluid density). The output of the MUT is acquired along with the necessary piston measurements so that average flows from the MUT and the flow standard can be compared.

Two types of piston arrangements are used in these systems. An *active* piston can both drive and measure a volumetric flow out of the cylinder (like a syringe), while a *passive* piston is pushed through the cylinder by pressure from a separate pump. The 0.1 L/s LFS employs a *passive* piston and the 2.5 L/s LFS employs an *active* piston.

NIST's LFSs were constructed by Flow Dynamics Inc, in Scottsdale, AZ[b] and the hardware and software updated in 2012 by Compuflow Solutions in Mesa, AZ[b]. Upon receipt at NIST, we calibrated the length, time, and temperature instruments and we measured the fluid properties necessary to make the system directly traceable to NIST standards. We analyzed the uncertainty of these standards and the results are documented herein.

The LFSs are operated in a closed loop mode. As shown schematically in Figure 2, the liquid is moved from the reservoir tank (by two pumps on the 0.1 L/s LFS and via a motor that moves the piston on the 2.5 LFS). The required flow passes through the piston-valve assembly and then to the test section, where the MUT is located. After the MUT, the entire flow is returned to the reservoir to complete the flow loop.

Two, three-way valves allow back and forth piston motion while maintaining unidirectional flow through the MUT, with brief pauses for changes in the piston direction. Calibration data is acquired with the piston moving in either direction.

Table 1. Nominal Characteristics of NIST's 0.1 L/s Liquid Flow Standard[c].

| | |
|---|---|
| Volume of the cylinder [$cm^3$], $V_p$ | 2229 |
| Diameter of the cylinder [cm], $D$ | 7.62 |
| Diameter of the piston shaft, [cm] $d$ | 2.54 |
| Length of the cylinder [cm], $L$ | 55 |
| Length of piston stroke [cm], $L_c$ | 14 to 55 |
| Duration of piston stroke [s], $t_c$ | 5 to 60 |
| Standard Uncertainty [%], $u_C$ | 0.022 |
| $U_{(95\ \%\ confidence\ level)}$, [%] | 0.044 |
| Volumetric flow range [L/s], $Q$, | 0.003 to 0.1 |

Table 2. Nominal Characteristics of NIST's 2.5 L/s Liquid Flow Standard[c].

| | |
|---|---|
| Volume of the cylinder [$cm^3$], $V_p$ | 21245 |
| Diameter of the cylinder [cm], $D$ | 15.24 |
| Diameter of the piston shaft, [cm] $d$ | 2.54 |
| Length of the cylinder [cm], $L$ | 120 |
| Length of piston stroke [cm], $L_c$ | 13 to 110 |
| Duration of piston stroke [s], $t_c$ | 1.4 to 200 |
| Standard Uncertainty[%], $u_C$ | 0.032 |
| $U_{(95\ \%\ confidence\ level)}$, [%] | 0.064 |
| Volumetric flow range [L/s], $Q$, | 0.02 to 2.0 |

c All values shown are within the uncertainty of the analyses shown in Section 5.

**A)** Photograph of the 0.1 L/s LFS.

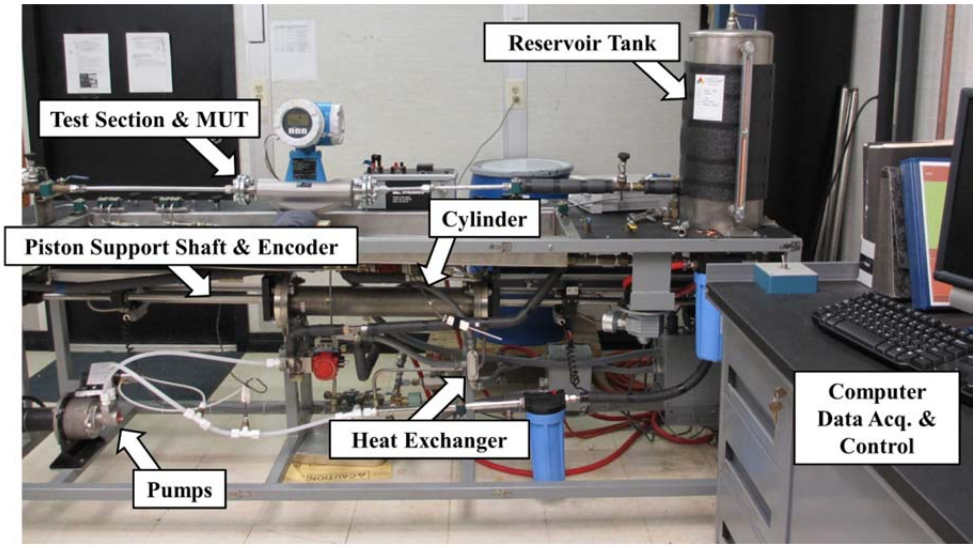


**B)** Photograph of the 2.5 L/s LFS.

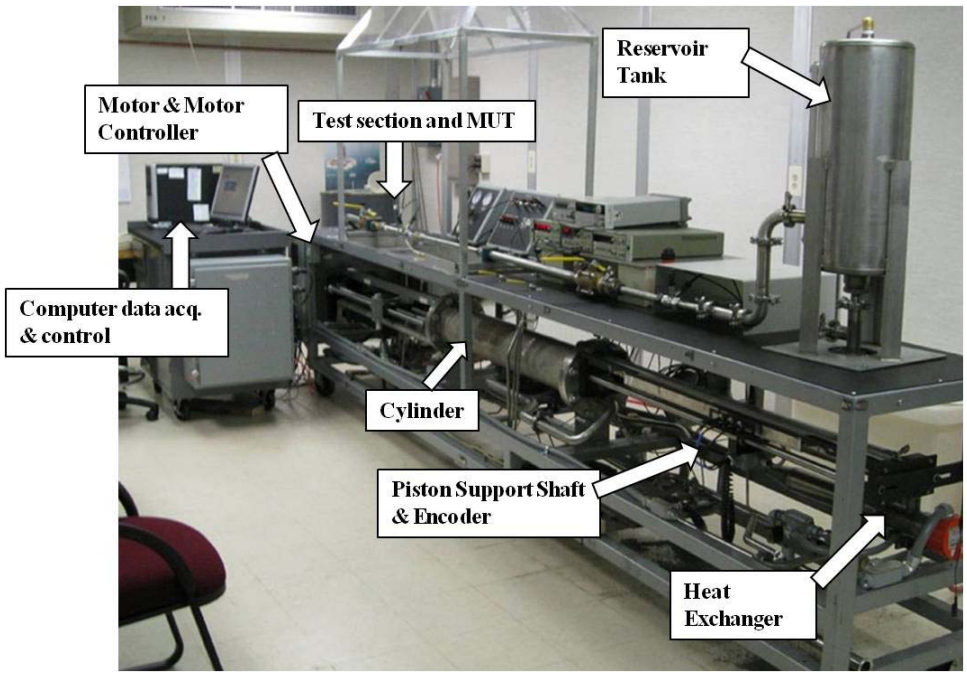


Figure 1. NIST's LFSs.

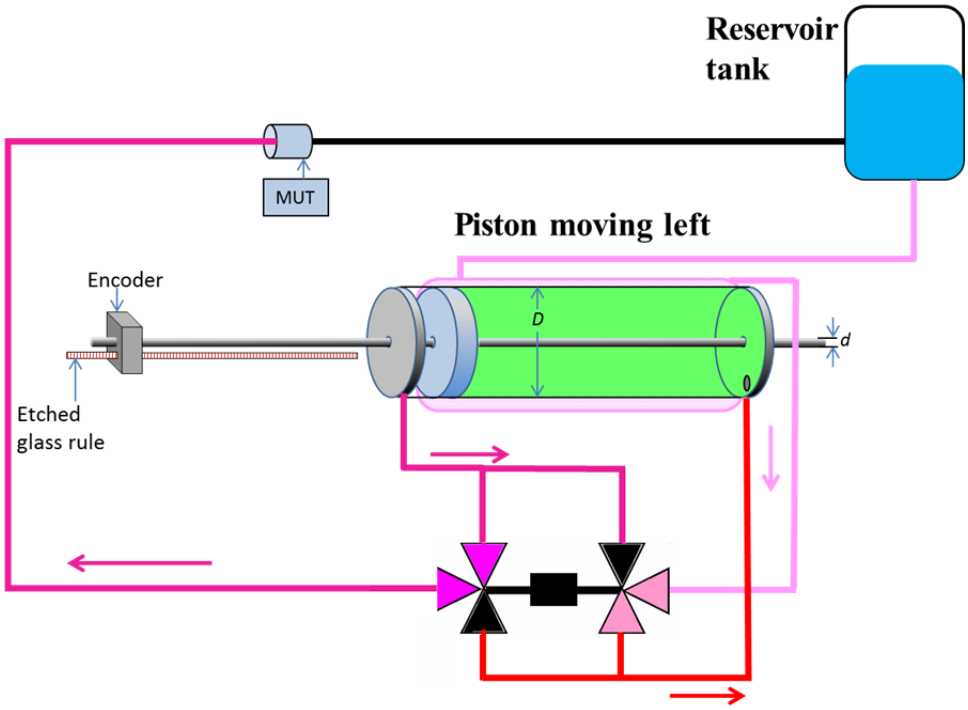


Figure 2. Sketch of the LFSs with the piston stroking left.

The operation of the four-way diverter valve is demonstrated schematically in Figures 2 and 3. The calibration interval begins as soon as flow conditions reach steady state and the piston accelerates to constant velocity (shortly after the piston begins travel in one direction). During the transition period when the piston changes direction, both of the three-way valves are set so that all three ports are open, thus preventing any hydraulic ram effects. During the change in direction, flow stops at the MUT, and it is necessary to wait for steady state conditions before beginning to collect calibration data. The meter output averaging is stopped before the piston reaches the transition period. To assure steady flow is achieved prior to taking a data point, data is acquired for the specified time for a given flow and stability in the MUT is evaluated. The MUT meter factor must be stable within 0.2 %. Once this stability is achieved, data is acquired only while this stability is maintained. When the piston changes direction, this stability criterion must be met again before another data point is taken.

To allow a range of flows, a computer-controlled stepping-motor drives both pumps on the 0.1 L/s LFS and the motor that moves the piston is computer-controlled on the 2.5 L/s LFS. The 0.1 L/s LFS capacity of the small pump is about one tenth the larger one. At lower flow conditions, the flow from the large pump is bypassed to the reservoir tank.

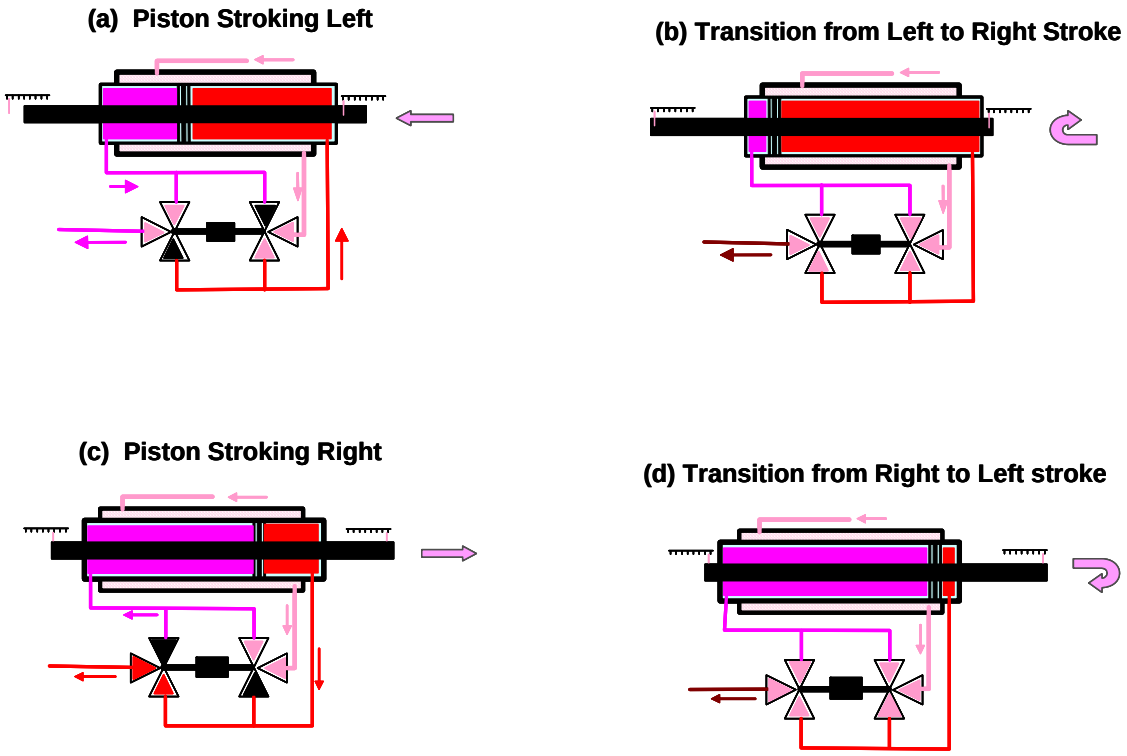


Figure 3. Diagrams of piston and three-way valves reversing piston directions.

Both LFSs are located in a temperature-controlled room where the air temperature is maintained at 21 ± 1.5 °C. Therefore, steady state temperature conditions are achieved by cycling the piston back and forth at the intended calibration flow, which promotes mixing of the fluid. Thermal equilibrium on the 0.1 L/s LFS is further enhanced by forcing the calibration fluid through an outer cylindrical jacket that encloses the cylinder and piston. The liquid flow from the pumps is directed into this outer jacket before entering the four-way diverter valve. The 0.1 L/s LFS uses twelve temperature sensors to determine fluid properties throughout the flow loop. The 2.5 L/s LFS uses ten temperature sensors and four pressure sensors. Placement of these sensors measures changes in density in the connecting volume between the cylinder and the MUT and the resulting corrections for storage effects. This is discussed further in section 5.

The position of the piston along the cylinder length is measured with two, redundant linear encoders, one on each of the supporting shafts attached to either side of the piston. The encoders output approximately 50 square wave pulses per mm of length traveled. The time for the piston to travel a given length is measured by counting pulses from two redundant 2.5 MHz timers (see section 5.2).

Leaks of calibration fluid can be visually detected. There are two wiper seals on the piston, one on the leading edge, another on the trailing edge. Fluid that leaks past either of these seals flows through machined holes in the piston and piston shafts to the shaft ends where it will drip out. Leaks past the piston shaft seals and from pipe fittings are easy to

detect by eye. Because leaks are detected and repaired, errors resulting from undetected leaks are small enough to be neglected during uncertainty analysis. To determine if a visible leak is significant, a graduated cylinder is used to collect the leaking fluid during the collection of a calibration flow point. If the collected volume is a large enough percentage of the volume through the MUT to increase the uncertainty in the measurement by more than 50 parts in $10^6$, it is repaired before the LFS is used again.

### 4.1 Flow Measurement Principle

Flow determinations are based on the piston displacing a known volume of fluid during a measured time interval. The volumetric flow exiting the cylinder is

$$Q_{\text{cyl}} = \frac{K_{\text{V}} N_{\text{e}}}{\Delta t} \tag{1}$$

where $K_{\text{V}}$ is the LFS constant or herein called the *volumetric prover K-factor* with units of volume per encoder pulse and $N_{\text{e}}$ is the number of encoder pulses. The volumetric prover *K*-factor equals[d]

$$K_{\text{V}} = A_{\text{cs}} \Delta L'_{\text{e}} \tag{2}$$

the cross sectional area $A_{\text{cs}}$ multiplied by the encoder constant $L'_{\text{e}}$. $K_{\text{V}}$ has slight dependence on the fluid operating temperature and pressure and on the room temperature. At different operating conditions, thermal expansion and pressure loading change the cylinder diameter ($D$) and the shaft diameter ($d$), and consequently $A_{\text{cs}}$. Similarly, thermal expansion causes $\Delta L'_{\text{e}}$ to change with the room temperature. Instead of characterizing $K_{\text{V}}$ over the range of prover operating conditions, standard practice is to determine its value at a single reference temperature ($T_{\text{ref}}$) and pressure ($P_{\text{ref}}$), and correct volumetric flow calculations for *reference condition effects* using

$$D = D_{\text{ref}}\left[1 + \alpha_{\text{st}}\left(T - T_{\text{ref}}\right)\right], \tag{3a}$$

$$d = d_{\text{ref}}\left[1 + \alpha_{\text{st}}\left(T - T_{\text{ref}}\right)\right], \tag{3b}$$

d The diameters of the shafts on either side of the piston are slightly different so that the cross sectional area differs slightly when the piston sweeps to the left versus to the right. To accommodate this difference it is not unusual to distinguish the value of the volumetric prover $K_{\text{V}}$ when the piston sweeps left ($K_{\text{V,left}}$) from when the piston sweeps right ($K_{\text{V,right}}$). In the case of the NIST LFSs, the differences between the left and right values are <0.01 % and can be neglected.

$$\Delta L'_{\mathrm{e}} = \Delta L'_{\mathrm{e,ref}}\left[1 + \alpha_{\mathrm{en}}\left(T_{\mathrm{en}} - T_{\mathrm{ref}}\right)\right] \tag{3c}$$

where $\alpha_{\mathrm{st}} = 1.7 \times 10^{-5}\ \mathrm{K}^{-1}$ [9,10] and $\alpha_{\mathrm{en}} = 8 \times 10^{-6}\ \mathrm{K}^{-1}$ [9] are the linear expansion coefficients for the stainless steel shafts and cylinder and for the glass encoder scale respectively. $T_{\mathrm{en}}$ and $T$ are the temperatures of the encoder and the fluid respectively.[e] Elastic deformation caused by pressure stresses can be neglected because the cylinder's cross-sectional area changes by less 4 parts in $10^6$ at the maximum operating pressure.[f] To minimize the uncertainties introduced by the linear temperature approximation used in Equation (3), the LFSs' operating conditions should be maintained close to $T_{\mathrm{ref}}$ and $P_{\mathrm{ref}}$. In this way, the theoretically corrected reference condition effects are small relative to the measured $K_{\mathrm{v}}^{\mathrm{ref}}$ values.

The three commonly used methods to determine the reference volumetric prover *K*-factor ($K_{\mathrm{v}}^{\mathrm{ref}}$) are 1) a water draw procedure [11], 2) dimensional measurements of the cylinder diameter ($D_{\mathrm{ref}}$), the shaft diameters on both sides of the piston ($d_{\mathrm{ref}}$), and the encoder constant ($\Delta L'_{\mathrm{e,ref}}$) [12], and 3) use of a transfer standard flow meter [11]. $K_{\mathrm{v}}^{\mathrm{ref}}$ was determined using the water draw method for the both LFSs. Dimensional measurements for the 0.1 L/s LFS have also been made for comparison with the water draw method. The water draw method is explained in section 5.2.

Flow at the MUT under Ideal Conditions

When the LFS is operated at the reference conditions, the volumetric flow exiting the cylinder is $Q_{\mathrm{cyl}}^{\mathrm{ref}} = K_{\mathrm{v}}^{\mathrm{ref}} N_{\mathrm{e}} / \Delta t$, and the mass flow is $\dot{m}_{\mathrm{cyl}}^{\mathrm{ref}} = \rho_{\mathrm{ref}} K_{\mathrm{v}}^{\mathrm{ref}} N_{\mathrm{e}} / \Delta t$ where $\rho_{\mathrm{ref}}$ is the fluid density evaluated at $P_{\mathrm{ref}}$ and $T_{\mathrm{ref}}$. The objective of a piston prover standard is to determine the flow at the MUT using theses reference flows. However, the volumetric and mass flow at the MUT only equal the respective reference flows (*i.e.*, $Q_{\mathrm{MUT}}^{\mathrm{ideal}} = Q_{\mathrm{cyl}}^{\mathrm{ref}}$ and $\dot{m}_{\mathrm{MUT}}^{\mathrm{ideal}} = \dot{m}_{\mathrm{cyl}}^{\mathrm{ref}}$) under the following idealized conditions:

1) steady flow,
2) room temperature equal to $T_{\mathrm{ref}}$,
3) fluid temperature equal to $T_{\mathrm{ref}}$ throughout the cylinder and test section,
4) fluid pressure equal to $P_{\mathrm{ref}}$ throughout the cylinder and test section, and

---

e The fluid temperature is assumed to be in thermal equilibrium with the cylinder and shaft, and the encoder temperature is assumed equal to the room temperature.

f At the maximum flow of the 2.5 L/s LFS the pressure at the outlet of the cylinder reaches 500 kPa. For this pressure, the percent of elastic deformation is calculated by: $100 \times 2\varepsilon_{\mathrm{eff}}(500 - 101.325)$, where $\varepsilon_{\mathrm{eff}}$ is the isothermal compressibility of stainless steel and has units of 1/kPa.

5) no leaks into or out of the piston-cylinder and test section.

NIST operates the LFSs as close as practical to these idealized conditions with the exception of the operating pressure. Steady flow conditions are obtained by using a tuned PID control to run the piston at a nearly constant velocity during data collection. Temperature uniformity of the fluid in the LFS assembly is established by cycling the piston back and forth until the multiple temperature sensors distributed throughout the test section and the 2 temperature sensors located at the left and right exits of the piston-cylinder assembly agree to within 0.5 C or better. The room housing the LFS is maintained to within ± 1 ºC of the reference temperature to minimize heat transfer effects. The pressure is maintained slightly above $P_{ref}$ (*i.e.*, 200 kPa or more, $P_{ref}$ = 101.325 kPa) to prevent measurement errors and possible damage caused by cavitation to customer turbine meters.

Corrections for Non-Ideal Operating Conditions

The ideal flow conditions listed above are never perfectly realized in practice. To improve flow measurement accuracy, corrections are made to $Q_{MUT}^{ideal}$ and $\dot{m}_{MUT}^{ideal}$ to account for small deviations from ideal conditions. In particular, corrections are made to account for non-idealities caused 1) by *reference condition effects*, 2) by *gradient effects* (*i.e.*, spatial non-uniformities in the temperature and/or pressure) and 3) *mass storage* effects (*i.e.* liquid density changes in the connecting volume between the cylinder and the MUT).

Corrections for reference condition effects are made when the operating conditions (*i.e.*, fluid temperature, fluid pressure, and room temperature) differ from $T_{ref}$ and $P_{ref}$. These corrections account either for changes in the cylinder volume or for changes in the fluid density. Reference condition corrections for fluid density are calculated using a linear function of temperature and pressure

$$\rho = \rho_{ref}\left[1 - \beta\left(T - T_{ref}\right) + \kappa\left(P - P_{ref}\right)\right] \tag{4}$$

where $\beta$ is the thermal expansion coefficient and $\kappa$ is the isothermal compressibility factor (or the inverse of the isothermal bulk modulus).

Pressure and temperature differences between the fluid exiting the cylinder and the fluid at the MUT cause the volumetric flow at these two locations to differ. These *gradient effects* are caused by pressure loss mechanisms such as wall friction, elbows, fittings, etc., as well as by heat transfer caused by temperature differences between the fluid and the room. Gradient effects are corrected by measuring the temperature and pressure at the cylinder exit and at the MUT. The measured temperatures and pressures are used in Equation (4) to calculate the density at the cylinder exit ($\rho_{cyl}$) and at the

MUT ($\rho_{MUT}$). Based on mass conservation, the volumetric flow at the MUT is taken to be equal to the volumetric flow at the cylinder multiplied by the density ratio ($\rho_{cyl}/\rho_{MUT}$).

A third type of non-ideality results from *mass storage effects* in the connecting volume between the swept cylinder volume and the MUT. For example, if the temperature of the fluid in the connecting volume drops between the start and stop of the averaging period, the density of the fluid in the connecting volume increases giving so-called mass storage there. In this case, the mass flow exiting the cylinder is greater than the mass flow reaching the MUT.[g] NIST corrects for *mass storage effects* in the 0.1 L/s LFS from known temperature changes during a measurement, but not for pressure changes. However, for each calibration we estimate the magnitude of these pressure effects and include them in the uncertainty budget. The *mass storage effects* are fully corrected for in the 2.5 L/s LFS. For both of NIST's LFSs, these corrections are < 4.3 parts in $10^6$.

Formulation of Governing Flow Equations

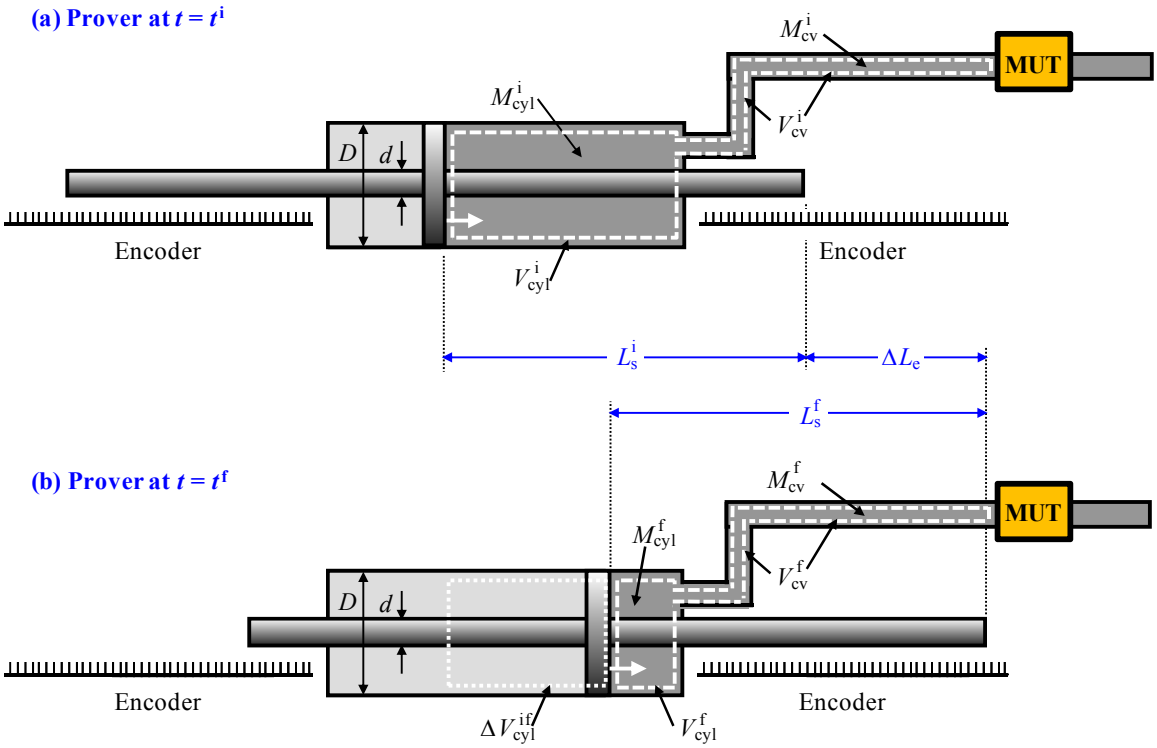


Figure 4. Sketch showing the orientation of the piston before and after the piston stroke.

g In the case of increasing connecting volume temperature the opposite occurs: more mass flow reaches the MUT than left the cylinder swept volume.

Figures 4a and 4b show the location of the piston at the start of the measured time interval ($t_\mathrm{i}$) and at the end of the measured time interval ($t_\mathrm{f}$). The white dashed lines constitute the *control volume* where mass conservation is applied. The control volume includes the volume of fluid to the right of the piston inside the cylinder ($V_\mathrm{cyl}$), and the fluid in the connecting volume between the exit of the cylinder and the MUT ($V_\mathrm{cv}$). As the piston strokes rightward the size of the control volume decreases such that the time-averaged mass flow through the MUT is:

$$\tilde{\dot{m}}_\mathrm{MUT} = \frac{\Delta M_\mathrm{cyl}^\mathrm{if}}{\Delta t} + \frac{\Delta M_\mathrm{cv}^\mathrm{if}}{\Delta t} - \tilde{\dot{m}}_\mathrm{leak} \ , \tag{5}$$

where $\Delta M_\mathrm{cyl}^\mathrm{if} = M_\mathrm{cyl}^\mathrm{i} - M_\mathrm{cyl}^\mathrm{f}$ is the difference between the initial and final mass in the cylinder, $\Delta M_\mathrm{cv}^\mathrm{if} = M_\mathrm{cv}^\mathrm{i} - M_\mathrm{cv}^\mathrm{f}$ is the difference between the initial and final mass in the connecting volume, $\Delta t = t_\mathrm{f} - t_\mathrm{i}$ is the measured time interval, and $\tilde{\dot{m}}_\mathrm{leak}$ is net time-averaged mass flow leaking out of the control volume. Alternatively, the mass terms in Equation (5) can be expressed

$$\tilde{\dot{m}}_\mathrm{MUT} = \frac{\hat{\rho}_\mathrm{cyl}^\mathrm{i} V_\mathrm{cyl}^\mathrm{i} - \hat{\rho}_\mathrm{cyl}^\mathrm{f} V_\mathrm{cyl}^\mathrm{f}}{\Delta t} + \frac{\hat{\rho}_\mathrm{cv}^\mathrm{i} V_\mathrm{cv}^\mathrm{i} - \hat{\rho}_\mathrm{cv}^\mathrm{f} V_\mathrm{cv}^\mathrm{f}}{\Delta t} - \tilde{\dot{m}}_\mathrm{leak}$$

or

$$\tilde{\dot{m}}_\mathrm{MUT} = \left[\frac{\hat{\rho}^\mathrm{i} V^\mathrm{i} - \hat{\rho}^\mathrm{f} V^\mathrm{f}}{\Delta t}\right]_\mathrm{cyl} + \left[\frac{\hat{\rho}^\mathrm{i} V^\mathrm{i} - \hat{\rho}^\mathrm{f} V^\mathrm{f}}{\Delta t}\right]_\mathrm{cv} - \tilde{\dot{m}}_\mathrm{leak} \tag{6}$$

as density multiplied by volume (*e.g.*, $M_\mathrm{cyl}^\mathrm{i} = \hat{\rho}_\mathrm{cyl}^\mathrm{i} V_\mathrm{cyl}^\mathrm{i}$, $M_\mathrm{cv}^\mathrm{i} = \hat{\rho}_\mathrm{cv}^\mathrm{i} V_\mathrm{cv}^\mathrm{i}$).[h] By adding and subtracting the terms $\hat{\rho}_\mathrm{cyl}^\mathrm{i} V_\mathrm{cyl}^\mathrm{f}$ and $\hat{\rho}_\mathrm{cv}^\mathrm{i} V_\mathrm{cv}^\mathrm{f}$ to the right side of Equation (6) the time-averaged mass flow (with no leaks) is

$$\tilde{\dot{m}}_\mathrm{MUT} = \left[\frac{\hat{\rho}^\mathrm{i} V^\mathrm{i} - \hat{\rho}^\mathrm{f} V^\mathrm{f} + \left(\hat{\rho}^\mathrm{i} V^\mathrm{f} - \hat{\rho}^\mathrm{i} V^\mathrm{f}\right)}{\Delta t}\right]_\mathrm{cyl} + \left[\frac{\hat{\rho}^\mathrm{i} V^\mathrm{i} - \hat{\rho}^\mathrm{f} V^\mathrm{f} + \left(\hat{\rho}^\mathrm{i} V^\mathrm{f} - \hat{\rho}^\mathrm{i} V^\mathrm{f}\right)}{\Delta t}\right]_\mathrm{cv}$$

h Note that $\hat{\rho}$ is the spatially averaged density.

$$= \left[ \frac{\left(\hat{\rho}^{\mathrm{i}} V^{\mathrm{i}} - \hat{\rho}^{\mathrm{i}} V^{\mathrm{f}}\right) + \left(\hat{\rho}^{\mathrm{i}} V^{\mathrm{f}} - \hat{\rho}^{\mathrm{f}} V^{\mathrm{f}}\right)}{\Delta t} \right]_{\mathrm{cyl}} + \left[ \frac{\left(\hat{\rho}^{\mathrm{i}} V^{\mathrm{i}} - \hat{\rho}^{\mathrm{i}} V^{\mathrm{f}}\right) + \left(\hat{\rho}^{\mathrm{i}} V^{\mathrm{f}} - \hat{\rho}^{\mathrm{f}} V^{\mathrm{f}}\right)}{\Delta t} \right]_{\mathrm{cv}}$$

$$= \left[ \frac{\hat{\rho}^{\mathrm{i}} \Delta V^{\mathrm{if}} + \Delta\hat{\rho}^{\mathrm{if}} V^{\mathrm{f}}}{\Delta t} \right]_{\mathrm{cyl}} + \left[ \frac{\hat{\rho}^{\mathrm{i}} \Delta V^{\mathrm{if}} + \Delta\hat{\rho}^{\mathrm{if}} V^{\mathrm{f}}}{\Delta t} \right]_{\mathrm{cv}}$$

$$= \frac{\hat{\rho}^{\mathrm{i}}_{\mathrm{cyl}} \Delta V^{\mathrm{if}}_{\mathrm{cyl}}}{\Delta t} + \frac{V^{\mathrm{f}}_{\mathrm{cyl}} \Delta\hat{\rho}^{\mathrm{if}}_{\mathrm{cyl}}}{\Delta t} + \frac{\hat{\rho}^{\mathrm{i}}_{\mathrm{cv}} \Delta V^{\mathrm{if}}_{\mathrm{cv}}}{\Delta t} + \frac{V^{\mathrm{f}}_{\mathrm{cv}} \Delta\hat{\rho}^{\mathrm{if}}_{\mathrm{cv}}}{\Delta t}$$

$$\widetilde{\dot{m}}_{\mathrm{MUT}} = \left( \frac{\hat{\rho}^{\mathrm{i}}_{\mathrm{cyl}} \Delta V^{\mathrm{if}}_{\mathrm{cyl}}}{\Delta t} \right) \left[ 1 + \frac{V^{\mathrm{f}}_{\mathrm{cyl}}}{\Delta V^{\mathrm{if}}_{\mathrm{cyl}}} \frac{\Delta\hat{\rho}^{\mathrm{if}}_{\mathrm{cyl}}}{\hat{\rho}^{\mathrm{i}}_{\mathrm{cyl}}} + \frac{V^{\mathrm{f}}_{\mathrm{cv}}}{\Delta V^{\mathrm{if}}_{\mathrm{cyl}}} \frac{\Delta\hat{\rho}^{\mathrm{if}}_{\mathrm{cv}}}{\hat{\rho}^{\mathrm{i}}_{\mathrm{cyl}}} + \frac{\hat{\rho}^{\mathrm{i}}_{\mathrm{cv}}}{\hat{\rho}^{\mathrm{i}}_{\mathrm{cyl}}} \frac{\Delta V^{\mathrm{if}}_{\mathrm{cv}}}{\Delta V^{\mathrm{if}}_{\mathrm{cyl}}} \right] \tag{7}$$

where $\Delta V^{\mathrm{if}}_{\mathrm{cyl}} = V^{\mathrm{i}}_{\mathrm{cyl}} - V^{\mathrm{f}}_{\mathrm{cyl}}$ is the volume swept by the piston during the measurement interval indicated by the dotted lines in Figure 4b. The terms in the square brackets account for mass storage in the portion of the cylinder volume not swept by the piston ($V^{\mathrm{f}}_{\mathrm{cyl}}$) shown in Figure 4b, and in the connecting volume ($V_{\mathrm{cv}}$).[i] Here, $\Delta\hat{\rho}^{\mathrm{if}}_{\mathrm{cyl}} = \hat{\rho}^{\mathrm{i}}_{\mathrm{cyl}} - \hat{\rho}^{\mathrm{f}}_{\mathrm{cyl}}$ and $\Delta\hat{\rho}^{\mathrm{if}}_{\mathrm{cv}} = \hat{\rho}^{\mathrm{i}}_{\mathrm{cv}} - \hat{\rho}^{\mathrm{f}}_{\mathrm{cv}}$ are the density differences in the unswept cylinder volume and in the connecting piping between the start and stop of a flow measurement. Similarly, $\Delta V^{\mathrm{if}}_{\mathrm{cv}} = V^{\mathrm{i}}_{\mathrm{cv}} - V^{\mathrm{f}}_{\mathrm{cv}}$ is the change in the connecting volume between the start and stop of a flow measurement.

The time-averaged volumetric flow at the MUT is determined by dividing Equation (7) by the time-averaged density at the MUT ($\widetilde{\rho}_{\mathrm{MUT}}$)

$$\widetilde{Q}_{\mathrm{MUT}} = \left( \frac{\Delta V^{\mathrm{if}}_{\mathrm{cyl}}}{\Delta t} \right) \left[ \frac{\hat{\rho}^{\mathrm{i}}_{\mathrm{cyl}}}{\widetilde{\rho}_{\mathrm{MUT}}} + \frac{V^{\mathrm{f}}_{\mathrm{cyl}}}{\Delta V^{\mathrm{if}}_{\mathrm{cyl}}} \frac{\Delta\hat{\rho}^{\mathrm{if}}_{\mathrm{cyl}}}{\widetilde{\rho}_{\mathrm{MUT}}} + \frac{V^{\mathrm{f}}_{\mathrm{cv}}}{\Delta V^{\mathrm{if}}_{\mathrm{cyl}}} \frac{\Delta\hat{\rho}^{\mathrm{if}}_{\mathrm{cv}}}{\widetilde{\rho}_{\mathrm{MUT}}} + \frac{\hat{\rho}^{\mathrm{i}}_{\mathrm{cv}}}{\widetilde{\rho}_{\mathrm{MUT}}} \frac{\Delta V^{\mathrm{if}}_{\mathrm{cv}}}{\Delta V^{\mathrm{if}}_{\mathrm{cyl}}} \right] - \frac{\widetilde{\dot{m}}_{\mathrm{leak}}}{\widetilde{\rho}_{\mathrm{MUT}}} . \tag{8}$$

As expected, both Equation (7) and Equation (8) simplify to $\dot{m}^{\mathrm{ideal}}_{\mathrm{MUT}} = \dot{m}^{\mathrm{ref}}_{\mathrm{cyl}}$ and $Q^{\mathrm{ideal}}_{\mathrm{MUT}} = Q^{\mathrm{ref}}_{\mathrm{cyl}}$ for the ideal operating conditions.

---

i Note that the unswept portion of the cylinder volume $V^{\mathrm{f}}_{\mathrm{cyl}}$ could be considered a portion of the connecting volume, but herein the quantity $V_{\mathrm{cv}}$ refers to only the fixed portion of the control volume.

Mass Flow and Volumetric Flow at the MUT

Equations (7) and (8) for the MUT mass flow and volumetric flow can be compactly expressed by

$$\tilde{\dot{m}}_{\mathrm{MUT}} = \left( \frac{\rho_{\mathrm{ref}} K_{\mathrm{V}}^{\mathrm{ref}} N_{\mathrm{e}}}{\Delta t} \right) R_1 R_2 R_3 R_4 R_5 S_1 S_2 S_3 S_4 S_5 S_6 \tag{9a}$$

and

$$\tilde{Q}_{\mathrm{MUT}} = \left[ \frac{K_{\mathrm{V}}^{\mathrm{ref}} N_{\mathrm{e}}}{\Delta t} \right] R_1 R_2 R_3 S_1 S_2 S_3 \, S_4 S_5 S_6 G_1 G_2 \tag{9b}$$

where the near unity correction factors indicated by the $R_{\mathrm{i}}$'s, $G_{\mathrm{i}}$'s, and $S_{\mathrm{i}}$'s account for *reference condition corrections*, *gradient corrections*, and *storage corrections*, respectively. The $R_{\mathrm{i}}$'s, correct the fluid density and the measured cylinder volume to the reference conditions. The $G_{\mathrm{i}}$'s correct the flow when pressure and temperature gradients exist between the piston-cylinder assembly and the MUT. The $S_{\mathrm{i}}$'s are mass *storage* corrections to account for differences in the unswept portion of the cylinder and connecting volume between the start and stop of a flow measurement. Expressions for these correction factors are given in Table 3 along with a description of their physical meaning. Note that the list of correction terms for the mass flow and volume flow in Equations (9a) and (9b) are not the same.

Many of the correction factors listed in Table 3 are essentially unity for the NIST operating conditions and do not affect flow calculations. Nevertheless, these correction factors have been retained to provide guidance for applications when operating conditions cannot be maintained close to the reference conditions. For example, some operators of piston provers vary fluid properties by changing fluid (and prover) temperature. For clarity, we specify correction factors that can be neglected when using Equations (9a) and (9b) for room temperature applications in the remaining sections of the manuscript.

The $S_{\mathrm{i}}$ correction factors in Table 3 show the need to measure temperature and pressure at $t_{\mathrm{i}}$ and at $t_{\mathrm{f}}$ to correct for storage effects. Moreover, the time response of the pressure and temperature instrumentation should be sufficiently fast to resolve transients. However, for NIST operating conditions, the difference in density of the cylinder fluid from the reference conditions ($R_4$) is by far the most significant correction factor for both LFSs. Its value is estimated by monitoring the temperature at the LFS cylinder outlet during a calibration. Typically, the temperature at the outlet of the cylinder is within 1 °C of the reference temperature (21 °C) such that $R_4 < 0.03$ %.

Table 3. Correction factors for mass flow in Equation (9a) and volumetric flow in Equation (9b).

| Region of LFS where correction applies | Equation | Type of correction | Description |
|---|---|---|---|
| Encoder | $R_1 = 1 + \alpha_{en}\left(T_{en} - T_{ref}\right)$ | *Reference* condition | Axial change in encoder scale length from reference due to thermal expansion |
| Displaced volume | $R_2 = 1 + 2\ \alpha_{st}\left(\hat{T}^{i}_{cyl} - T_{ref}\right)$ [j] | *Reference* condition | Radial change in the cylinder and the shaft diameter from reference conditions due to internal fluid pressure. |
| Displaced volume | $R_3 = 1 + 2\ \varepsilon_{eff}\left(\hat{P}^{i}_{cyl} - P_{ref}\right)$ | *Reference* condition | Radial change in cylinder and shaft diameter from the reference condition due to internal fluid pressure[k] |
| Displaced volume | $R_4 = 1 - \beta\left(\hat{T}^{i}_{cyl} - T_{ref}\right)$ | *Reference* condition | Change in the fluid density from the reference density ($\rho_{ref}$) due to thermal expansion |
| Displaced volume | $R_5 = 1 + \kappa\left(\hat{P}^{i}_{cyl} - P_{ref}\right)$ | *Reference* condition | Change in the fluid density from the reference density ($\rho_{ref}$) due to pressure difference from $P_{ref}$ |
| Displaced volume/MUT | $G_1 = 1 - \beta\left(\hat{T}^{i}_{cyl} - \widetilde{T}_{MUT}\right)$ [l] | Temperature *Gradient* | Ratio density change between cylinder and MUT attributed to temperature difference between the cylinder and MUT |
| Displaced volume/MUT | $G_2 = 1 + \kappa\left(\hat{P}^{i}_{cyl} - \widetilde{P}_{MUT}\right)$ | Pressure *Gradient* | Ratio density change between cylinder and MUT attributed to pressure difference between the cylinder and MUT |

j $\hat{T}$ and $\hat{P}$ are the spatially averaged temperature and pressure, respectively.

k Note that $\varepsilon_{eff}$ and $\varepsilon_{cv}$ are parameters with units of inverse pressure to be determined using the appropriate pressure vessel equations in terms of the material modulus of elasticity, Poisson ratio, and dimensions.

l $\widetilde{T}$ and $\widetilde{P}$ are the time averaged temperature and pressure, respectively.

Continuation of Table 3.

| Region of LFS where correction applies | Equation | Type of correction | Description |
|---|---|---|---|
| Upswept Volume of Cylinder | $S_1 = 1 + 2\left(\frac{V_{\text{cyl}}^{\text{f}}}{N_{\text{e}} K_{\text{V}}^{\text{ref}}}\right)\alpha_{\text{st}}\left(\hat{T}_{\text{cyl}}^{\text{i}} - \hat{T}_{\text{cyl}}^{\text{f}}\right)$ | Mass *Storage* | Radial change in the unswept region of the cylinder and shaft diameters due to a temperature change between the start and stop of a calibration |
| Upswept Volume of Cylinder | $S_2 = 1 + 2\left(\frac{V_{\text{cyl}}^{\text{f}}}{N_{\text{e}} K_{\text{V}}^{\text{ref}}}\right)\varepsilon_{\text{eff}}\left(\hat{P}_{\text{cyl}}^{\text{i}} - \hat{P}_{\text{cyl}}^{\text{f}}\right)$ | Mass *Storage* | Radial change in the unswept region of the cylinder and shaft diameters due to a pressure change between the start and stop of a calibration |
| Upswept Volume of Cylinder | $S_3 = 1 - \left(\frac{V_{\text{cyl}}^{\text{f}}}{N_{\text{e}} K_{\text{V}}^{\text{ref}}}\right)\beta\left(\hat{T}_{\text{cyl}}^{\text{i}} - \hat{T}_{\text{cyl}}^{\text{f}}\right)$ | Mass *Storage* | Change in the fluid density in the unswept region of the cylinder due to a temperature change between the start and stop of a calibration |
| Upswept Volume of Cylinder | $S_4 = 1 + \left(\frac{V_{\text{cyl}}^{\text{f}}}{N_{\text{e}} K_{\text{V}}^{\text{ref}}}\right)\kappa\left(\hat{P}_{\text{cyl}}^{\text{i}} - \hat{P}_{\text{cyl}}^{\text{f}}\right)$ | Mass *Storage* | Change in the fluid density in the unswept region of the cylinder due to a pressure change between the start and stop of a calibration |
| Connecting volume | $S_5 = 1 + \left(\frac{V_{\text{cv}}^{\text{ref}}}{N_{\text{e}} K_{\text{V}}^{\text{ref}}}\right)\left(3\alpha_{\text{cv}} - \beta\right)\left(\hat{T}_{\text{cv}}^{\text{i}} - \hat{T}_{\text{cv}}^{\text{f}}\right)$ | Mass *Storage* | Change in the connecting volume and the density of fluid in this region due to a temperature change between the start and stop of a calibration |
| Connecting volume | $S_6 = 1 + \left(\frac{V_{\text{cv}}^{\text{ref}}}{N_{\text{e}} K_{\text{V}}^{\text{ref}}}\right)\left(2\varepsilon_{\text{cv}} + \kappa\right)\left(\hat{P}_{\text{cv}}^{\text{i}} - \hat{P}_{\text{cv}}^{\text{f}}\right)$ | Mass *Storage* | Mass storage in connecting volume attributed to pressure difference between start and stop of flow measurement |

## 5.0 Uncertainty Analysis Overview

The uncertainty components of the LFSs are discussed in detail in following sections. As seen in Equations (9a) and (9b), they include the uncertainty of the following elements:

a. volumetric prover *K*-factor ( $K_{\text{V}}^{\text{ref}}$ ),

b. the displaced prover volume, $\Delta V_{\text{cyl}}$, the linear thermal expansion coefficient for the piping, $\alpha_{\text{S}}$,

c. temperature and pressure measurements at the MUT, the cylinder exit, and in the connecting volume,

d. the LFS cylinder and connecting volume, $V_{\text{cyl}}$, $V_{\text{CV}}$,

e. the calibration interval, $\Delta t_c$,

f. the thermal expansion coefficient of the liquid, $\beta$

g. and the isothermal compressibility factor of the liquid, $\kappa$.

Some component uncertainties listed above and in Equations (9a) and (9b) could not be measured directly. Their uncertainties are estimated from the uncertainties of their source measurements using the first order uncertainty propagation method to be discussed below. Figure 5 shows a graphic representation tree of the uncertainty analysis for the LFS.

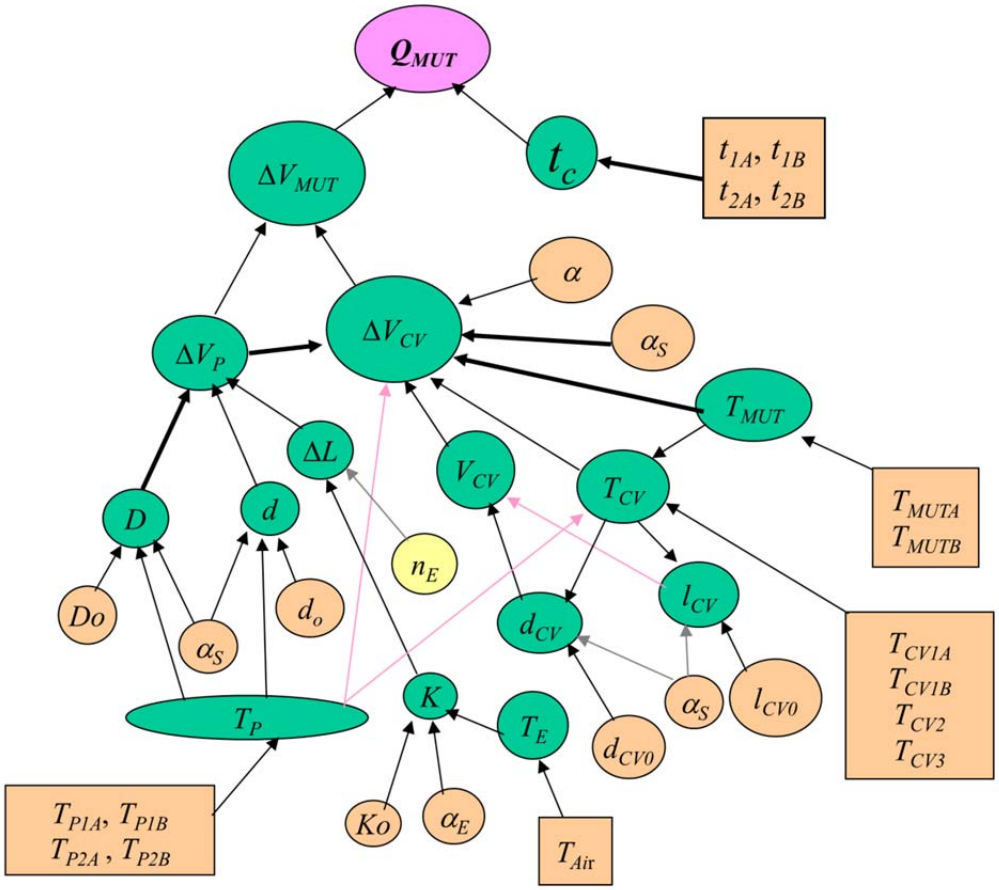


Figure 5. Graphic representation of the uncertainty analysis. The subscript "P" denotes the LFS's cylinder.

### 5.1 Techniques for Uncertainty Analysis

Here we follow the guidelines for evaluating and expressing uncertainty provided in NIST TN 1297 [13], the ISO Guide to Uncertainty in Measurement [3], and elsewhere [14]. In general, if a measurement quantity, $y$, is a function of variables $x_i$,

$$y = f(x_1, x_2, ....., x_n) \tag{10}$$

its first-order Taylor series approximation is,

$$dy = \sum_i \frac{\partial y}{\partial x_i} dx_i \tag{11}$$

Thus, the propagation of uncertainty yields

$$\begin{aligned} u_c^2(y) &= \left[ \sum_{i=1}^{n} \left( \frac{\partial y}{\partial x_i} \right) u(x_i) \right]^2 \\ &= \sum_{i=1}^{n} \left( \frac{\partial y}{\partial x_i} \right)^2 u^2(x_i) + 2 \sum_{i=1}^{n-1} \left( \frac{\partial y}{\partial x_i} \right) \sum_{j=i+1}^{n} \left( \frac{\partial y}{\partial x_j} \right) r_{ij} u(x_i) u(x_j) \end{aligned} \tag{12}$$

where $u_c(y)$ is the combined standard uncertainty of the measurement result $y$, $u(x_i)$ is the standard uncertainty of the variable $x_i$, the partial derivatives $\partial y / \partial x_i$ are the dimensional sensitivity coefficients of $x_i$ on $y$, and $r_{ij}$ is the cross correlation coefficient between variables $x_i$ and $x_j$. An alternative form of Equation (12), which expresses the uncertainty propagation in a dimensionless form, is shown below and it is often more useful.

$$u_y^2 = \sum_{i=1}^{n} c_{x_i}^2 u_{x_i}^2 + 2 \sum_{i=1}^{n-1} \sum_{j=i+1}^{n} c_{x_i} c_{x_j} \; r_{ij} \; u_{x_i} u_{x_j} \tag{13}$$

In Equation (13), $u_y = u_c(y) / y$ is the combined dimensionless standard uncertainty of the measurement result $y$, $c_{x_i} = (\partial y / \partial x_i) \, x_i / y$ are the dimensionless sensitivity coefficients of $x_i$ on $y$, and $u_{x_i} = u(x_i) / x_i$ is the dimensionless uncertainty of the variable $x_i$. Equation (13) is used here to estimate the combined uncertainty of the measurement. In many cases, the uncertainty of $x_i$ could not be measured directly. For those cases, the same uncertainty propagation given by Equation (13) is used for a sub-measurement process to estimate the combined uncertainty of the sub-measurement. This process is propagated throughout all the measurement components needed until the desired measured quantities are obtained.

According to [3], the sources of uncertainty used in assessing the combined standard uncertainty of the measurement process can be classified according to two types: *Type A* - those which are evaluated by statistical methods, and *Type B* - those which are evaluated by other means. Following this convention, each measured quantity has been classified accordingly as a $u_A$ or $u_B$.

### 5.2 Measured Quantities and Their Uncertainties

The method of propagation of uncertainty was used to determine the uncertainties of: 1) $K_V^{ref}$ determined by the water draw procedure, 2) the volumetric flow at the MUT, and 3) the mass flow at the MUT. For each of these quantities the relevant uncertainty sources are taken to be uncorrelated. Standard uncertainties (*i.e.*, 68 % confidence level) are multiplied by their normalized sensitivity coefficients and root-sum-squared (RSS) to determine the expanded uncertainties (or approximate 95 % confidence level).

Determination of and Uncertainty of the Volumetric Prover *K*-factor ( $K_V^{ref}$ )

The reference volumetric prover *K*-factor ( $K_V^{ref}$ ) for both LFSs was determined using a water draw procedure at a reference temperature and pressure of $T_{ref}$ = 21 ºC and $P_{ref}$ = 101.325 kPa. First, an empty collection vessel was weighed using the substitution method with reference masses calibrated by the NIST mass group. The vessel and reference masses were weighed five times. After temperature equilibrium was established in both the room and the fluid, the piston was slowly traversed through the cylinder and the displaced fluid was directed into the collection vessel instead of through the MUT. Following the collection, the vessel was again weighed five times using the substitution method with reference masses. Thus, we determine $K_V^{ref}$ using Equation (9a) for totalized mass flow. However, the total mass that would have passed through the MUT (*i.e.*, $\tilde{\dot{m}}_{MUT}\,\Delta t$) is replaced by the buoyancy corrected and calibrated substitution method weigh scale readings as shown in:

$$K_V^{ref} = \frac{\left(W^f - W^i\right)\left(1 + \rho_{air}/\rho_{ref}\right)}{N_e \rho_{ref}\left(\prod_{n=1}^{5} R_n\right)\left(\prod_{n=1}^{6} S_n\right)}\,, \tag{14}$$

where $W^i$ is the weight (or apparent mass) of the empty collection vessel and $W^f$ is the final weight after filling the collection vessel, and the quantity $\left(1 + \rho_{air}/\rho_{ref}\right)$ is the buoyancy correction. The air density ( $\rho_{air}$ ) is calculated as a function of the pressure, temperature, and relative humidity in the room using the correlation developed by Jaeger and Davis [15]. During the $K_V^{ref}$ measurement, the room temperature was controlled to within ± 1°C of $T_{ref}$, the fluid

temperature was controlled to within ± 0.5°C of $T_{ref}$, and the fluid pressure was 100 kPa ± 9 kPa. For these conditions $R_4 = 1 - \beta(\hat{T}^{i}_{cyl} - T_{ref})$ is the only significant correction factor. All of the other reference condition and storage corrections attribute less than 5 parts in $10^6$ to $K_V^{ref}$ .

The 2.5 L/s LFS $K_V^{ref}$ was measured on multiple occasions via the water draw method (Figure 6). Measurements were done with the piston stroking to the left ( $K_{V,left}^{ref}$ ) and then with the piston stroking right ( $K_{V,right}^{ref}$ ). On each occasion, $K_{V,left}^{ref}$ and $K_{V,right}^{ref}$ were measured a minimum of 5 times each using Stoddard solvent or reverse osmosis water as the working fluid. The difference between $K_{V,left}^{ref}$ and $K_{V,right}^{ref}$ is less than 50 parts in $10^6$ for the multiple measurements, *i.e.*, the two shaft diameters are nearly equal. Based on this good agreement, the average $K_V^{ref}$ can be used for both directions without significant increase in the uncertainty, *i. e.* $K_V^{ref} = (K_{V,left}^{ref} + K_{V,left}^{ref})/2$ . The $K_V$ of the 2.5 L/s LFS has been measured on eight occasions since 2008 and they all agree within 540 parts in $10^6$.

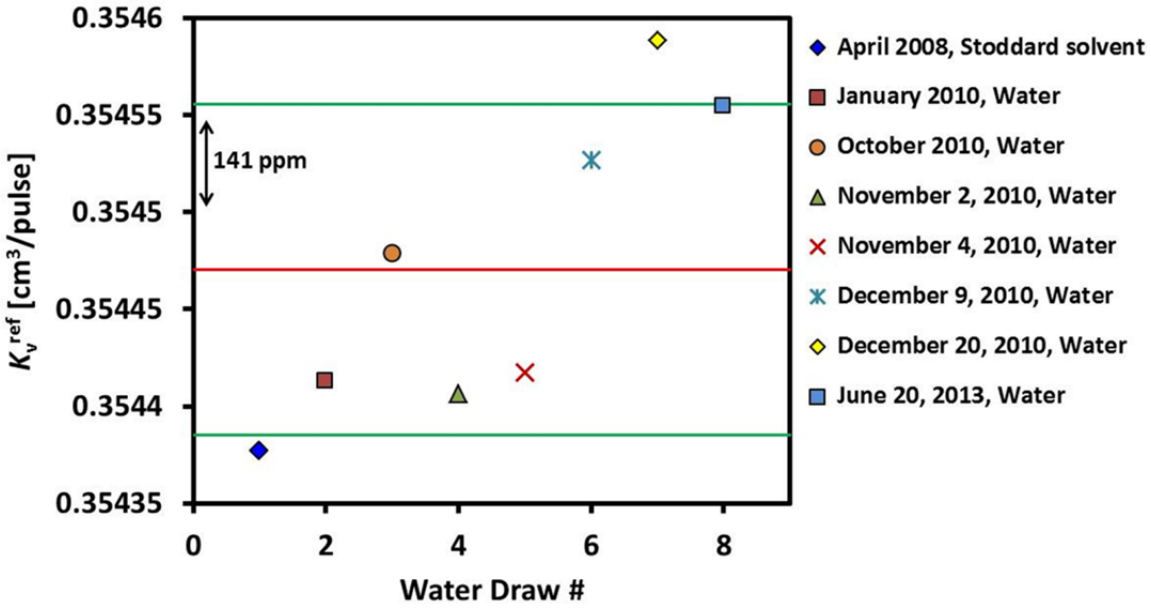


Figure 6. Plot showing measurements of $K_V^{ref}$ for the 2.5 L/s LFS done in Stoddard solvent (April 2008) and in water purified by reverse osmosis. The upper and lower lines represent the 95 % confidence interval. The middle line represents the average of the measurements.

The 0.1 L/s LFS $K_V^{ref}$ was measured on two occasions, one via dimensional analysis in 2005 and one time via the water draw method in April of 2013 (Figure 7). The difference between the two values is < 140 parts in $10^6$. The details for the dimensional analysis can be found in the prior version of the NIST Special Publication for this calibration service [16]. During the 2013 water draw, five measurements were made with the piston stroking to the left ($K_{V,left}^{ref}$) and five measurements with the piston stroking right ($K_{V,right}^{ref}$) with reverse osmosis water as the working fluid. The difference between $K_{V,left}^{ref}$ and $K_{V,right}^{ref}$ was less than 40 parts in $10^6$ and therefore negligible. It is worth noting that Figure 6 and Figure 7 show the average $K_V^{ref}$ from two linear encoders. However, in practice the two encoder length scales are not exactly equal (50 μm/pulse is the nominal value) and there are two $K_V^{ref}$ values used, one for each encoder. Because of the relative ease in performing a water draw compared to a dimensional analysis, the water draw method will be used in the future to verify $K_V^{ref}$ when needed.

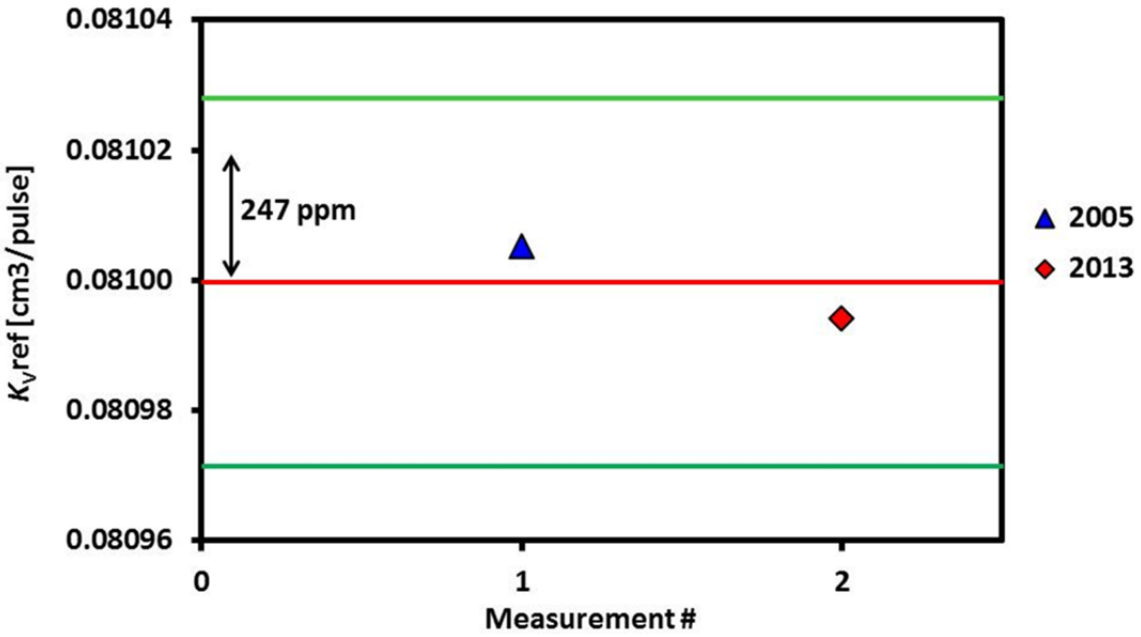


Figure 7. Plot showing measurements of $K_V^{ref}$ for the 0.1 L/s LFS. The $K_V^{ref}$ measurement in 2005 is from dimensional analysis. The $K_V^{ref}$ measurements in April 2013 are via the water draw method using water purified by reverse osmosis. The upper and lower lines represent the 95 % confidence interval. The middle line represents the average of the measurements.

The expression used to calculate the uncertainty of the measured $K_V^{ref}$ by the water draw method is given by Equation (15):

$$\left[\frac{u(K_V^{ref})}{K_V^{ref}}\right]^2 = \left[\frac{W^i}{K_V^{ref}}\frac{\partial K_V^{ref}}{\partial W^i}\right]^2\left[\frac{u(W^i)}{W^i}\right]^2 + \left[\frac{W^f}{K_V^{ref}}\frac{\partial K_V^{ref}}{\partial W^f}\right]^2\left[\frac{u(W^f)}{W^f}\right]^2 + \left[\frac{\beta}{K_V^{ref}}\frac{\partial K_V^{ref}}{\partial \beta}\right]^2\left[\frac{u(\beta)}{\beta}\right]^2$$

$$+\left[\frac{\rho_{ref}}{K_V^{ref}}\frac{\partial K_V^{ref}}{\partial \rho_{ref}}\right]^2\left[\frac{u(\rho_{ref})}{\rho_{ref}}\right]^2 + \left[\frac{\rho_{air}}{K_V^{ref}}\frac{\partial K_V^{ref}}{\partial \rho_{air}}\right]^2\left[\frac{u(\rho_{air})}{\rho_{air}}\right]^2 + \left[\frac{\rho_{ref.mass}}{K_V^{ref}}\frac{\partial K_V^{ref}}{\partial \rho_{ref.mass}}\right]^2\left[\frac{u(\rho_{ref.mass})}{\rho_{ref.mass}}\right]^2 \quad (15)$$

$$+\left[\frac{N_e}{K_V^{ref}}\frac{\partial K_V^{ref}}{\partial N_e}\right]^2\left[\frac{u(N_e)}{N_e}\right]^2 + \left[\frac{\hat{T}_{cyl}^i}{K_V^{ref}}\frac{\partial K_V^{ref}}{\partial \hat{T}_{cyl}^i}\right]^2\left[\frac{u(\hat{T}_{cyl}^i)}{\hat{T}_{cyl}^i}\right]^2 + \frac{\sigma_{Kv}^2}{N} + \frac{\sigma_W^2}{N},$$

where $\sigma_{Kv}$ is the standard deviation of the repeated measurements and $\sigma_W$ is the standard deviation of the repeated weighing's of reference masses and the full and empty collection vessel. Tables 4 and 5 show the uncertainty budget for $K_V^{ref}$ for the 0.1 L/s LFS and the 2.5 L/s LFS respectively.

Table 4. Uncertainty budget for $K_V^{ref}$ corresponding to Equation (15) for the 0.1 L/s LFS.

| **Vol. Prover *K*-factor**<br>**$K_v^{ref}$ = 0.08099 [cm$^3$/pulse]**<br>**Uncertainty Category** | **Nom. Value** | **Rel. Unc. ($k$ = 1) [%]** | **Norm. Sen. Coeff. ($c$) [-]** | **Type A/B** | **Contribution [%]** | **Comments** |
|---|---|---|---|---|---|---|
| **Reference masses** | 1521 g | 0.0008 | 1 | B | 0.7 | From NIST Mass Group cal report |
| **Reference mass density** | 7.8 g/cm$^3$ | $1.0 \times 10^{-6}$ | 0.00015 | B | <0.001 | From mass manufacturer |
| **Room air density** | 0.0012 g/cm$^3$ | 0.050 | 0.00105 | B | < 0.001 | Instrument cal records |
| **Water density, $\rho_{ref}$** | 0.99803 g/cm$^3$ | 0.005 | -1 | B | 29.5 | Density of water used in draw. |
| **Thermal Expan. Coeff. For water, $\beta$, [1/°C]** | 0.0002 | 0.003 | -0.0001 | A | <0.001 | From best fit line to cal data from 19 °C to 23 °C |
| **Encoder Pulses, $N_e$, [pulse]** | 12350 | 0.0023 | -1 | B | 6.4 | Integer number of pulses. One pulse may be missed, rectangular distribution assumed |
| **Initial Fluid Temp, $T^i_{cyl}$, [°C]** | 20.52 | 0.02 | 0.059 | B | 1.0 | From spatial average of temperature sensors |
| **Repeated measurement of "small" reference masses, $\sigma/\sqrt{n}$** | N/A | $2.9 \times 10^{-4}$ | 1 | A | 0.10 | Standard deviation of mean, 5 measurements |
| **Repeated measurement of "large" reference masses, $\sigma/\sqrt{n}$** | N/A | $8.1 \times 10^{-5}$ | 1 | A | 0.008 | Standard deviation of mean, 5 measurements |
| **Repeated measurement of empty container, $\sigma/\sqrt{n}$** | N/A | $2.8 \times 10^{-4}$ | 1 | A | 0.09 | Standard deviation of mean, 5 measurements |
| **Repeated measurement of full container, $\sigma/\sqrt{n}$** | N/A | $3.7 \times 10^{-4}$ | 1 | A | 0.16 | Standard deviation of mean, 5 measurements |
| **Repeated measurement of $K_v^{ref}$, $\sigma/\sqrt{n}$** | 0.08099 | 0.0019 | 1 | A | 4.3 | Standard deviation of mean, 10 measurements |
| **Reproducibility of multiple $K_v^{ref}$, $\sigma/\sqrt{n}$** | 0.081 | 0.0070 | 1 | A | 57.8 | Long term reproducibility of the measurement |
| **Combined Standard Uncertainty ($k$ = 1) [%]** | **0.009** | | | | | |

Table 5. Uncertainty budget for $K_V^{ref}$ corresponding to Equation (15) for the 2.5 L/s LFS.

| **Vol. Prover *K*-factor**<br>**$K_v^{ref}$ = 0.35432 [cm$^3$/pulse]**<br>**Uncertainty Category** | **Nom. Value** | **Rel. Unc. ($k$ = 1) [%]** | **Norm. Sen. Coeff. ($c$) [-]** | **Type A/B** | **Contribution [%]** | **Comments** |
|---|---|---|---|---|---|---|
| **Reference masses** | 7900 g | 0.0006 | 1 | B | 0.3 | From NIST Mass Group cal report |
| **Reference mass density** | 7.8 g/cm$^3$ | $1.0 \times 10^{-6}$ | 0.00015 | B | <0.001 | From mass manufacturer |
| **Room air density** | 0.0012 g/cm$^3$ | 0.050 | 0.00105 | B | 0.002 | Instrument cal records |
| **Water density, $\rho_{ref}$** | 0.99836 g/cm$^3$ | 0.005 | -1 | B | 17.2 | Density of water used in draw. |
| **Thermal Expan. Coeff. For water, $\beta$, [1/°C]** | 0.0002 | 0.003 | -0.0001 | A | <0.001 | From best fit line to cal data from 19 °C to 23 °C |
| **Encoder Pulses, *Ne*, [pulse]** | 15000 | 0.0019 | -1 | B | 2.6 | Integer number of pulses. One pulse may be missed, rectangular distribution assumed |
| **Initial Fluid Temp, $T^i_{cyl}$, [°C]** | 20.5 | 0.04 | 0.059 | B | 4.1 | From spatial average of temperature sensors |
| **Repeated measurement of "small" reference masses, $\sigma/\sqrt{n}$** | 1230 g | $7.9 \times 10^{-5}$ | 1 | A | 0.004 | Standard deviation of mean, 5 measurements |
| **Repeated measurement of "large" reference masses, $\sigma/\sqrt{n}$** | 6590 g | $7.0 \times 10^{-5}$ | 1 | A | 0.003 | Standard deviation of mean, 5 measurements |
| **Repeated measurement of empty container, $\sigma/\sqrt{n}$** | 1229 g | $5.8 \times 10^{-4}$ | 1 | A | 0.23 | Standard deviation of mean, 5 measurements |
| **Repeated measurement of full container, $\sigma/\sqrt{n}$** | 6590 g | $1.1 \times 10^{-4}$ | 1 | A | 0.01 | Standard deviation of mean, 5 measurements |
| **Repeated measurement of $K_v^{ref}$, $\sigma/\sqrt{n}$** | 0.35455 | 0.0031 | 1 | A | 6.6 | Standard deviation of mean, 10 measurements |
| **Reproducibility of multiple $K_v^{ref}$, $\sigma/\sqrt{n}$** | 0.35445 | 0.01 | 1 | A | 69.0 | Long term reproducibility of the measurement |
| **Combined Standard Uncertainty ($k$ = 1) [%]** | **0.012** | | | | | |

Temperature Measurement

The uncertainty of the temperature measurements made throughout the LFS will contribute to the uncertainty of the calibrator. Platinum resistance temperature detectors (RTDs) are used for all temperature measurements, with twelve and ten of them placed at various locations along the liquid flow path on the 0.1 L/s and the 2.5 L/s LFS respectively. At locations deemed critical, the systems have duplicate sensors to improve measurement accuracy.

The model used for the reduction of the various temperatures in the system affects the uncertainty of the LFS results. At initial and final conditions, the average connecting volume fluid temperature, $T_{CV}$ , is assumed to be the average value of the five temperature readings (each LFS has five RTDs along the connecting volume) made along the fluid path.

$$T_{CV} = \left(T_P + T_{CV1} + T_{CV2} + T_{CV3} + T_{MUT}\right) / 5 . \tag{16}$$

Typical temperature variation in the connecting volume of the 2.5 L/s LFS during a meter calibration is shown in Figure 8. The LFS starts the calibration at the flow (2.0 L/s) such that the friction within the LFS warms the fluid by approximately 0.2 K, following this warming as the flow decreases the temperature change diminishes. This and other test data show that the maximum temperature change over time or difference between any two sensors among the sensor locations is 0.4 K or less during a data collection interval. The NIST LFSs have the capability of taking the temperature (and pressure for the 2.5 L/s LFS) at the beginning and at the end of a data collection and corrections for gradient effects and mass storage effects are made, making uncertainties due to temporal variations in temperature negligible. Since 5 temperature sensors are distributed in the connecting volume, spatial temperature uncertainties are negligible too. However, if the initial and final temperatures (and pressure) are not known, the temporal uniformity of the temperature sensors during a calibration can be used as a guide to assign an uncertainty to gradient and mass storage effects. That is, the temperature change between data collection intervals can give insight to the values of the initial and final temperatures. For example, if temperature control in a standard is poor and only the average temperature during a flow point is recorded, the rate of change of the temperature between data points can be used as a guide in determining what the initial and final temperatures are. For illustration purposes, Figure 9 shows the temperature in a fictitious flow standard that is not well controlled. Data points are taken every 30 seconds and the temperature is changing by 2 K between consecutive flow points. Therefore, it can be assumed that the temperature change during the collection of a flow point is as high as 0.07 K/s. The time of the flow point collection multiplied by this rate of change will give an approximation of the change in initial and final temperatures during the collection and hence an uncertainty can be assigned.

The RTDs are calibrated annually in an isothermal bath by comparing their response to that of a standard thermometer calibrated by the NIST Thermometry Group. The three to four calibration coefficients and the temperature uncertainty for each RTD are obtained using a linear regression method. The uncertainty in the reference temperature, which is 0.002 K,

is classified as a Type B uncertainty for each RTD. During calibration of the RTDs, a minimum of five data points are collected at each temperature set point. The root-sum-square of the uncertainties from the reference sensor, the sample standard deviation of the measurements at each set point, the data regression, and the sensor drift over its calibration interval gives the combined uncertainty of each RTD. In the worst case, the RTDs have $u_A = 0.041$ K and $u_B = 0.031$ K.

Pressure Measurements

Unlike the 2.5 L/s system, the 0.1 L/s LFS does not have pressure transducers in multiple locations that allow corrections for the spatial and temporal changes in mass throughout the system. Therefore, pressure effects are treated as uncertainty components for the 0.1 L/s LFS. However, the 2.5 L/s LFS has been upgraded to have pressure transducers at the outlet of both sides of the cylinder, upstream of the MUT, and downstream of the MUT. These measurements allow us to make connecting volume and spatial non-uniformity corrections. Therefore, uncertainty of the pressure measurements made throughout the LFS will contribute to its overall uncertainty.

The pressure transducers are calibrated every five years against a pressure reference that is traceable to the NIST group responsible for pressure calibrations. The three to four calibration coefficients and the pressure uncertainty for each transducer are obtained using a linear regression method. The uncertainty in the reference pressure (0.01 %) is classified as a Type B uncertainty for each transducer. The root-sum-square of the uncertainties from the reference sensor, data regression, and estimated drift between calibrations gives the combined uncertainty of each transducer. In the worst case, the transducers have $u_A = 0.05$ % and $u_B = 0.033$ %.

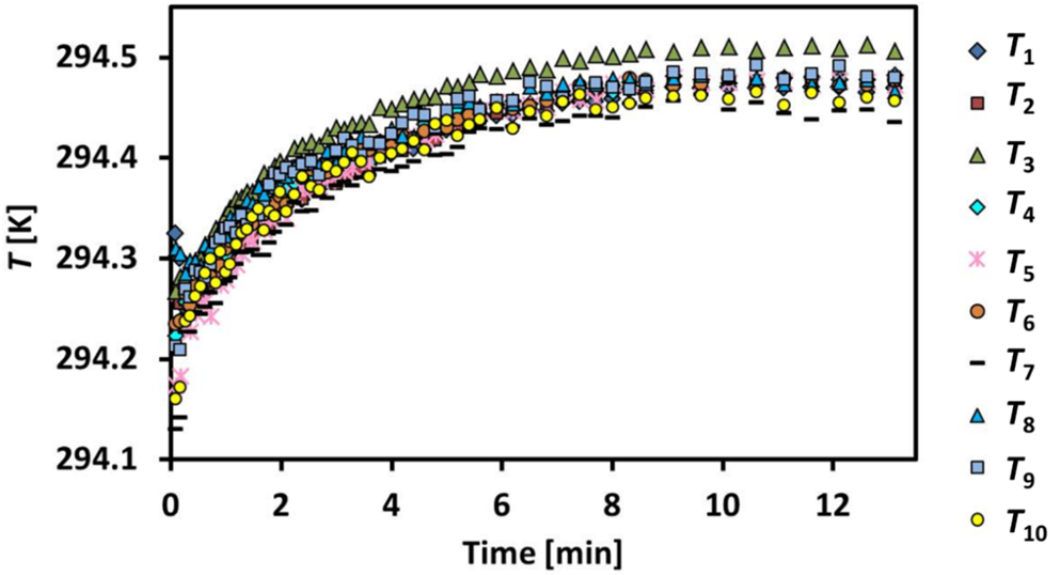


Figure 8. Temperature measurements made by the 10 sensors in the 2.5 L/s LFS during a calibration of six flow points with five repeats for each flow point. Temperature uniformity along the flow path is < 0.1 K and temporal stability at each location is < 0.4 K.

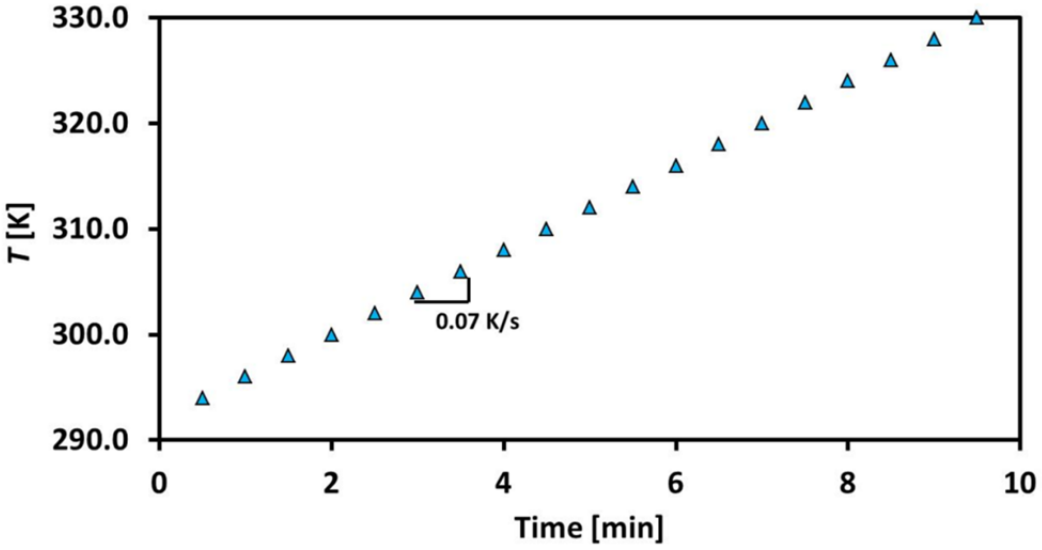


Figure 9. Temperatures in a fictitious flow standard to illustrate how to use the average temperature measurements made in a series of flow collections to predict initial and final temperatures for input to an uncertainty analysis.

The Connecting Volume

The connecting volume is modeled using the following equation:

$$V_{CV} = \pi \, d_{CV}^2 \, l_{CV} \, / \, 4 \tag{17}$$

In Equation (17), $d_{CV}$ is the averaged internal diameter of the connecting pipe and $l_{CV}$ is its length. There is significant uncertainty associated with the estimation of the quantities needed to compute the connecting volume: piping inside diameters, piping lengths, internal volumes of the valves and elbows, the unswept volume in the LFS, the extra connecting volumes associated with the piping used for different MUTs, etc. However, as shown in Tables 6 and 7 below, the sensitivity of the volumetric flow through the MUT to the connecting volume is quite small. The large uncertainty of the connecting volume will result only 0.1 part in $10^6$ of flow uncertainty in the case of the 0.1 L/s LFS. This is because the change in density of the fluid in the connecting volume during a flow measurement is small (the temperature profile is quite stable) and because the connecting volume is small in size compared to the volume swept out by the piston. Furthermore, the uncertainties related to dimensional changes of the control volume due to thermal expansion are even smaller and are neglected.

Time of Piston Displacement

The uncertainty of the measurements of time can be separated into two parts: a) that due to the reference clock (including calibration errors and temperature effects) and b) that due to quantization errors. The time base oscillators are periodically calibrated by two reference counters that are traceable to NIST time and frequency standards. The Type A uncertainty of the LFS oscillators used in this uncertainty analysis is 0.31 μHz/Hz and the Type B uncertainty is 1.55 μHz/Hz. These oscillator calibration uncertainties are larger than the quantization uncertainties discussed below.

Figure 10 illustrates that the quantization error for a generic timed interval will be smaller than or equal to one time reference unit (± $\Delta t$). The true time, $t_{true}$, is marked by the start and stop times, $t_1$ and $t_3$. The data acquisition system obtains the measured time, $t_{meas}$, by counting the number of rising edges, $n$, from the reference clock (nominally 2.5 MHz in this case) between $t_2$ and $t_4$ and multiplying $n$ by the reference time unit (0.4 μs). The timing errors at the start and end of the measurement ($\delta_s$ and $\delta_e$) can each be between zero and one time unit in magnitude. The resulting difference between the true and measured times is ± one time reference unit. The start and end timing errors each have rectangular probability distributions and the difference between them (the quantization error) has a standard uncertainty of $\Delta t/\sqrt{6}$. Although the example uses rising edges for triggering, this analysis is equally valid for falling edges. It does assume that no pulse is missed by the counter.

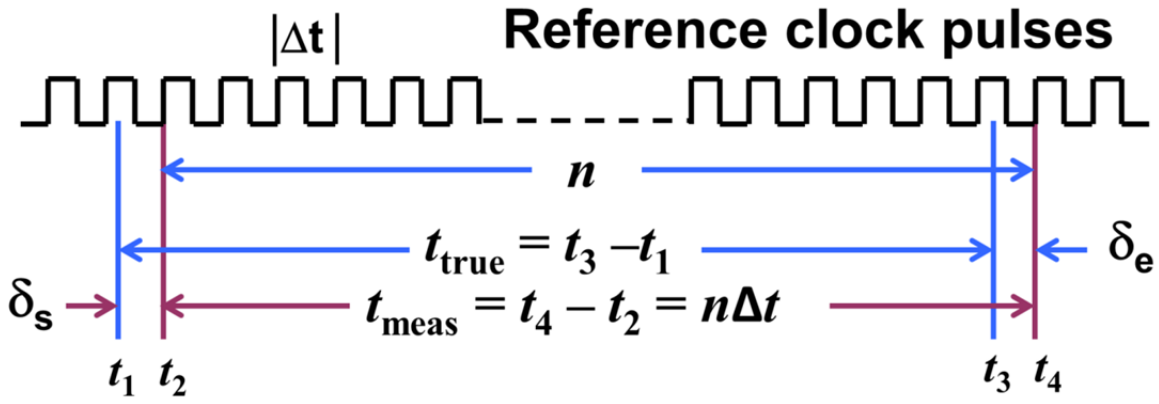


Figure 10. A sketch showing how reference clock pulses are used to time a generic interval and how the timing procedure leads to a quantization error of ± one time reference unit (± $\Delta t$).

Figure 11 illustrates the application of the reference clock to measurement of the time for the piston to travel a selected distance, as indicated by a selected number of pulses output by one of the encoders. The figure also illustrates the measurement of the frequency output by a MUT. Once the test conditions have reached steady state (at time $t_0$), the next rising edge output by the encoder is used to commence the counting of rising edges from the reference clock. After the predetermined number ($N_e$) of encoder pulses has been registered by a counter, the counting of reference clock pulses is

stopped, and the total ($N$) is multiplied by $\Delta t$ to obtain the time required by the piston to travel the prescribed distance ($t_{Emeas}$). As for the generic case, this time has a standard uncertainty due to quantization of $\Delta t/\sqrt{6}$.

The frequency of the flow meter output, $f_T$, is calculated by dividing the total number of pulses output ($N_T$) by the time between two rising edges of the flow meter output ($t_{Tmeas}$) that occur immediately after the encoder rising edges that mark the start and stop of the piston travel time. Note that the encoder time is measured independently from the flow meter time and while they are very nearly coincident, they are not necessarily equal in duration. As for the previous cases, the flow meter pulse totalization time has quantization uncertainty of $\Delta t/\sqrt{6}$.

The LFSs have redundancy in the encoders and oscillators in order to avoid miscounting pulses and to allow internal validation of measurements. Each LFS system uses two encoders (1 and 2), each providing two pulse outputs (A and B). Output A originates from the leading edges of the encoder pulses and output B indicates the trailing edges. Therefore, a total of four chronometries (1A, 1B, 2A, and 2B) are used to measure the piston travel and thereby improve the accuracy of the measured collection time. Additionally, the LFSs use two oscillators each to measure the piston travel interval. The first oscillator is used to measure time for chronometries 1A and 2A and the second oscillator operates on 1B and 2B. The Type B uncertainties of the clocks are assumed to be fully correlated between clocks operated by the same oscillator. Increasing the number of chronometries or measurements does not improve the measurement uncertainty when the uncertainties are fully correlated.

The fact that the intervals over which the encoder and flow MUT frequencies are measured are not perfectly coincident is a negligible uncertainty contributor because the time difference is < 0.001 % and the flow is steady within 0.2 %.

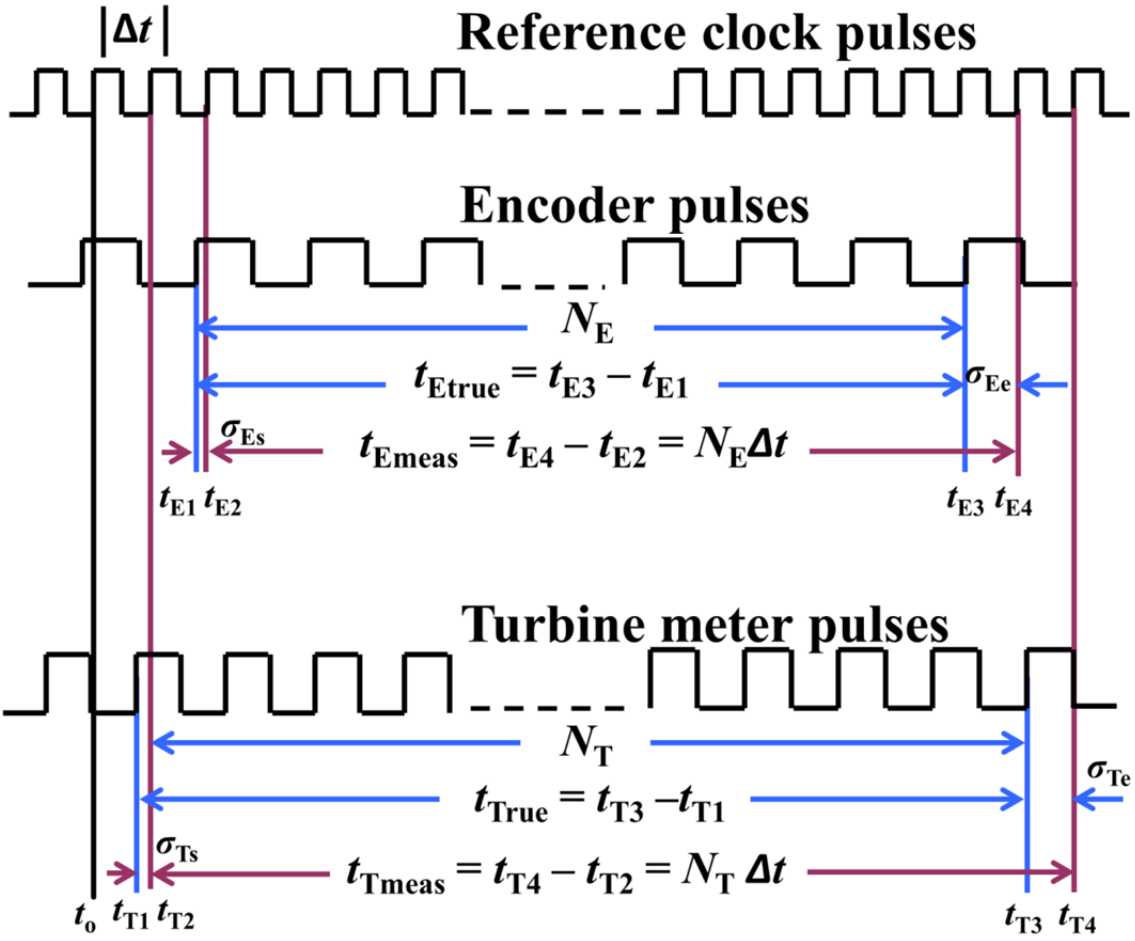


Figure 11. Diagram of the process for counting and timing the pulses from the encoder that measures piston displacement and from a pulse generating MUT (e.g., a turbine meter) and their quantization errors.

Fluid Properties

As indicated in Equation (9b), the thermal expansion and isothermal compressibility of the fluid, and not the density itself, affects the volumetric flow determination. The physical property values involved in the expression for fluid density as a function of temperature are periodically determined off-line, using an oscillating tube densitometer (calibrated with air, distilled water, and NIST Standard Reference Materials). Likewise, the fluid kinematic viscosity does not directly affect the flow results in this type of LFS. However, depending on the type of MUT, the fluid kinematic viscosity can affect the flow meter output [5,6]. For the report of calibration, the fluid viscosities are periodically measured using a falling ball viscometer which measures the time required for a ball of known dimensions to pass by two detectors a known distance apart through the fluid in a capillary tube of known diameter.

### 5.3 Propagating Components of Uncertainty

Referring to the graphic representation of the uncertainty analysis, given in Figure 5 and the uncertainty propagation Equation (13) given above, the uncertainty of the sub-measurements must be assessed before the flow uncertainty can be

estimated. This process is propagated throughout all the measurement components until the uncertainties of the desired quantities are obtained. After the uncertainties of the sub-measurements are obtained, the one-standard-deviation, ($k$ = 1), uncertainty for the volumetric flow as given in Equation (9b), is obtained via the square of the combined standard uncertainty of the volumetric flow at the MUT and is calculated by:

$$
\begin{aligned}
\left[\frac{u_c\left(\widetilde{Q}_{\mathrm{MUT}}\right)}{\widetilde{Q}_{\mathrm{MUT}}}\right]^2 = {} & \left(\frac{K_{\mathrm{V}}^{\mathrm{ref}}}{\widetilde{Q}_{\mathrm{MUT}}}\frac{\partial \widetilde{Q}_{\mathrm{MUT}}}{\partial K_{\mathrm{V}}^{\mathrm{ref}}}\right)^2\left[\frac{u\left(K_{\mathrm{V}}^{\mathrm{ref}}\right)}{K_{\mathrm{V}}^{\mathrm{ref}}}\right]^2 + \left(\frac{N_{\mathrm{e}}}{\widetilde{Q}_{\mathrm{MUT}}}\frac{\partial \widetilde{Q}_{\mathrm{MUT}}}{\partial N_{\mathrm{e}}}\right)^2\left[\frac{u\left(N_{\mathrm{e}}\right)}{N_{\mathrm{e}}}\right]^2 \\
& + \left(\frac{\Delta t}{\widetilde{Q}_{\mathrm{MUT}}}\frac{\partial \widetilde{Q}_{\mathrm{MUT}}}{\partial \Delta t}\right)^2\left[\frac{u\left(\Delta t\right)}{\Delta t}\right]^2 + \left(\frac{\widetilde{T}_{\mathrm{MUT}}}{\widetilde{Q}_{\mathrm{MUT}}}\frac{\partial \widetilde{Q}_{\mathrm{MUT}}}{\partial \widetilde{T}_{\mathrm{MUT}}}\right)^2\left[\frac{u\left(\widetilde{T}_{\mathrm{MUT}}\right)}{\widetilde{T}_{\mathrm{MUT}}}\right]^2 \\
& + \left(\frac{T_{\mathrm{en}}}{\widetilde{Q}_{\mathrm{MUT}}}\frac{\partial \widetilde{Q}_{\mathrm{MUT}}}{\partial T_{\mathrm{en}}}\right)^2\left[\frac{u\left(T_{\mathrm{en}}\right)}{T_{\mathrm{en}}}\right]^2 + \left(\frac{\hat{T}_{\mathrm{cyl}}^{\mathrm{i}}}{\widetilde{Q}_{\mathrm{MUT}}}\frac{\partial \widetilde{Q}_{\mathrm{MUT}}}{\partial \hat{T}_{\mathrm{cyl}}^{\mathrm{i}}}\right)^2\left[\frac{u\left(\hat{T}_{\mathrm{cyl}}^{\mathrm{i}}\right)}{\hat{T}_{\mathrm{cyl}}^{\mathrm{i}}}\right]^2 \\
& + \left(\frac{\hat{T}_{\mathrm{cyl}}^{\mathrm{f}}}{\widetilde{Q}_{\mathrm{MUT}}}\frac{\partial \widetilde{Q}_{\mathrm{MUT}}}{\partial \hat{T}_{\mathrm{cyl}}^{\mathrm{f}}}\right)^2\left[\frac{u\left(\hat{T}_{\mathrm{cyl}}^{\mathrm{f}}\right)}{\hat{T}_{\mathrm{cyl}}^{\mathrm{f}}}\right]^2 + \left(\frac{\hat{T}_{\mathrm{cv}}^{\mathrm{i}}}{\widetilde{Q}_{\mathrm{MUT}}}\frac{\partial \widetilde{Q}_{\mathrm{MUT}}}{\partial \hat{T}_{\mathrm{cv}}^{\mathrm{i}}}\right)^2\left[\frac{u\left(\hat{T}_{\mathrm{cv}}^{\mathrm{i}}\right)}{\hat{T}_{\mathrm{cv}}^{\mathrm{i}}}\right]^2 \\
& + \left(\frac{\hat{T}_{\mathrm{cv}}^{\mathrm{f}}}{\widetilde{Q}_{\mathrm{MUT}}}\frac{\partial \widetilde{Q}_{\mathrm{MUT}}}{\partial \hat{T}_{\mathrm{cv}}^{\mathrm{f}}}\right)^2\left[\frac{u\left(\hat{T}_{\mathrm{cv}}^{\mathrm{f}}\right)}{\hat{T}_{\mathrm{cv}}^{\mathrm{f}}}\right]^2 + \left(\frac{\widetilde{P}_{\mathrm{MUT}}}{\widetilde{Q}_{\mathrm{MUT}}}\frac{\partial \widetilde{Q}_{\mathrm{MUT}}}{\partial \widetilde{P}_{\mathrm{MUT}}}\right)^2\left[\frac{u\left(\widetilde{P}_{\mathrm{MUT}}\right)}{\widetilde{P}_{\mathrm{MUT}}}\right]^2 \\
& + \left(\frac{\hat{P}_{\mathrm{cyl}}^{\mathrm{i}}}{\widetilde{Q}_{\mathrm{MUT}}}\frac{\partial \widetilde{Q}_{\mathrm{MUT}}}{\partial \hat{P}_{\mathrm{cyl}}^{\mathrm{i}}}\right)^2\left[\frac{u\left(\hat{P}_{\mathrm{cyl}}^{\mathrm{i}}\right)}{\hat{P}_{\mathrm{cyl}}^{\mathrm{i}}}\right]^2 + \left(\frac{\hat{P}_{\mathrm{cyl}}^{\mathrm{f}}}{\widetilde{Q}_{\mathrm{MUT}}}\frac{\partial \widetilde{Q}_{\mathrm{MUT}}}{\partial \hat{P}_{\mathrm{cyl}}^{\mathrm{f}}}\right)^2\left[\frac{u\left(\hat{P}_{\mathrm{cyl}}^{\mathrm{f}}\right)}{\hat{P}_{\mathrm{cyl}}^{\mathrm{f}}}\right]^2 \\
& + \left(\frac{\hat{P}_{\mathrm{cv}}^{\mathrm{i}}}{\widetilde{Q}_{\mathrm{MUT}}}\frac{\partial \widetilde{Q}_{\mathrm{MUT}}}{\partial \hat{P}_{\mathrm{cv}}^{\mathrm{i}}}\right)^2\left[\frac{u\left(\hat{P}_{\mathrm{cv}}^{\mathrm{i}}\right)}{\hat{P}_{\mathrm{cv}}^{\mathrm{i}}}\right]^2 + \left(\frac{\hat{P}_{\mathrm{cv}}^{\mathrm{f}}}{\widetilde{Q}_{\mathrm{MUT}}}\frac{\partial \widetilde{Q}_{\mathrm{MUT}}}{\partial \hat{P}_{\mathrm{cv}}^{\mathrm{f}}}\right)^2\left[\frac{u\left(\hat{P}_{\mathrm{cv}}^{\mathrm{f}}\right)}{\hat{P}_{\mathrm{cv}}^{\mathrm{f}}}\right]^2 \\
& + \left(\frac{\rho_{\mathrm{ref}}}{\widetilde{Q}_{\mathrm{MUT}}}\frac{\partial \widetilde{Q}_{\mathrm{MUT}}}{\partial \rho_{\mathrm{ref}}}\right)^2\left[\frac{u\left(\rho_{\mathrm{ref}}\right)}{\rho_{\mathrm{ref}}}\right]^2 + \left(\frac{\beta}{\widetilde{Q}_{\mathrm{MUT}}}\frac{\partial \widetilde{Q}_{\mathrm{MUT}}}{\partial \beta}\right)^2\left[\frac{u\left(\beta\right)}{\beta}\right]^2 \\
& + \left(\frac{\alpha_{\mathrm{en}}}{\widetilde{Q}_{\mathrm{MUT}}}\frac{\partial \widetilde{Q}_{\mathrm{MUT}}}{\partial \alpha_{\mathrm{en}}}\right)^2\left[\frac{u\left(\alpha_{\mathrm{en}}\right)}{\alpha_{\mathrm{en}}}\right]^2 + \left(\frac{\alpha_{\mathrm{st}}}{\widetilde{Q}_{\mathrm{MUT}}}\frac{\partial \widetilde{Q}_{\mathrm{MUT}}}{\partial \alpha_{\mathrm{st}}}\right)^2\left[\frac{u\left(\alpha_{\mathrm{st}}\right)}{\alpha_{\mathrm{st}}}\right]^2 \\
& + \left(\frac{\kappa}{\widetilde{Q}_{\mathrm{MUT}}}\frac{\partial \widetilde{Q}_{\mathrm{MUT}}}{\partial \kappa}\right)^2\left[\frac{u\left(\kappa\right)}{\kappa}\right]^2 + \left(\frac{\varepsilon_{\mathrm{eff}}}{\widetilde{Q}_{\mathrm{MUT}}}\frac{\partial \widetilde{Q}_{\mathrm{MUT}}}{\partial \varepsilon_{\mathrm{eff}}}\right)^2\left[\frac{u\left(\varepsilon_{\mathrm{eff}}\right)}{\varepsilon_{\mathrm{eff}}}\right]^2 \\
& + \left(\frac{\varepsilon_{\mathrm{cv}}}{\widetilde{Q}_{\mathrm{MUT}}}\frac{\partial \widetilde{Q}_{\mathrm{MUT}}}{\partial \varepsilon_{\mathrm{cv}}}\right)^2\left[\frac{u\left(\varepsilon_{\mathrm{cv}}\right)}{\varepsilon_{\mathrm{cv}}}\right]^2 + \left(\frac{V_{\mathrm{cv}}}{\widetilde{Q}_{\mathrm{MUT}}}\frac{\partial \widetilde{Q}_{\mathrm{MUT}}}{\partial V_{\mathrm{cv}}}\right)^2\left[\frac{u\left(V_{\mathrm{cv}}\right)}{V_{\mathrm{cv}}}\right]^2 .
\end{aligned}
\tag{18}
$$

Table 6 itemizes each component of uncertainty for the 0.1 L/s LFS and Table 7 for the 2.5 L/s LFS.

Table 6. Uncertainty budget for volumetric flow at the MUT for the 0.1 L/s LFS corresponding to Equation (9b).

| **Vol. Flow; $Q_{MUT}$ [L/s]**<br>**$Q_{MUT}$ = 0.04 [L/s]**<br>**Uncertainty Category** | **Nom. Value** | **Rel. Unc. ($k$ = 1) [%]** | **Norm. Sen. Coeff. ($S_c$) [-]** | **Contribution [%]** | **Comments** |
|---|---|---|---|---|---|
| **Volumetric prover *K*-factor, $K_v$ [cm$^3$/pulse]** | 0.0810 | 0.009 | 1 | 50.9 | From water draw |
| **Encoder pulses, $N_{en}$ [pulse]** | 5000 | 0.0058 | 1 | 21.0 | Integer number of redundant pulses, one may be missed |
| **Duration of piston stroke, $\Delta t$ [s]** | 9 | 0.0002 | -1 | 0.025 | Control charts for freq. cal. |
| **Linear thermal expansion coefficient of piston, cylinder, shafts, $\alpha_{st}$ [1/°C]** | 0.000017 | 5 | $-1.6\times10^{-05}$ | 0.0042 | See reference [9, 10] |
| **Linear thermal expansion coefficient of encoder material, $\alpha_{en}$ [1/°C]** | 0.000008 | 5 | $-6\times10^{-06}$ | < 0.001 | See reference [9, 10] |
| **Fixed connecting volume (not including unswept cylinder volume), $V_{cv}$ [cm$^3$]** | 260 | 10 | $-4.2\times10^{-06}$ | 0.0011 | Calculated from LFS geometry measurements |
| **Linear thermal expansion coefficient of fixed connecting volume, $\alpha_{cv}$ [1/°C]** | 0.000017 | 5 | $8.54\times10^{-07}$ | < 0.001 | See references [9, 10] |
| **Variable connecting volume (*i.e.*, unswept cylinder volume), $V^f_{cyl}$ [cm$^3$]** | 1906 | 5 | $-9.3\times10^{-06}$ | 0.0014 | Calculated from LFS geometry measurements |
| **Encoder (and room) temperature, $T_{en}$ [°C]** | 20.25 | 0.030 | 0.0024 | 0.003 | Temperature cal records and data from LFS |
| **Initial liquid temperature in the cylinder, $T^i_{cyl}$ [°C]** | 20.52 | 0.017 | -0.29 | 15.1 | Temperature cal records and data from LFS |
| **Final liquid temperature in the cylinder, $T^f_{cyl}$ [°C]** | 20.53 | 0.017 | 0.24 | 10.1 | Temperature cal records and data from LFS |
| **Initial liquid pressure in the cylinder, $P^i_{cyl}$ [kPa]** | 110 | 4.5 | 0.00028 | 1.0 | Pressure cal records and data from LFS |
| **Final liquid pressure in the cylinder, $P^f_{cyl}$ [kPa]** | 115 | 4.3 | -0.00024 | 0.70 | Pressure cal records and data from LFS |

Continuation of Table 6.

| Uncertainty Category | Nom. Value | Rel. Unc. ($k$ = 1) [%] | Norm. Sen. Coeff. ($S_c$) [-] | Contribution [%] | Comments |
|---|---|---|---|---|---|
| **Initial liquid temperature in the fixed connecting volume, $T^{i}_{cv}$ [°C]** | 20.90 | 0.017 | -0.030 | 0.17 | Temperature cal records and data from LFS |
| **Final liquid temperature in the fixed connecting volume, $T^{f}_{cv}$ [°C]** | 20.87 | 0.017 | 0.030 | 0.17 | Temperature cal records and data from LFS |
| **Initial liquid pressure in the fixed connecting volume, $P^{i}_{cv}$ [kPa]** | 110 | 4.5 | $3.3\text{x}10^{-05}$ | 0.014 | Pressure cal records and data from LFS |
| **Final liquid pressure in the fixed connecting volume, $P^{f}_{cv}$ [kPa]** | 115 | 4.3 | $-3.5\text{x}10^{-05}$ | 0.014 | Pressure cal records and data from LFS |
| **Liquid temperature at the MUT, $T_{mut}$ [°C]** | 20.61 | 0.017 | 0.062 | 0.71 | Temperature cal records and data from LFS |
| **Liquid pressure at the MUT, $P_{mut}$ [kPa]** | 105 | 4.8 | $-4.8\text{x}10^{-05}$ | 0.033 | Pressure cal records and data from LFS |
| **Liquid volumetric thermal expansion coefficient, $\beta$ [1/°C]** | 0.00021 | 3.3 | $2\text{x}10^{-05}$ | 0.003 | Derived from Temperature/density relationship determined by NIST. |
| **Liquid isothermal compressibility factor, $k$ [1/kPa]** | $4.6\text{x}10^{-07}$ | 20 | $-9.5\text{x}10^{-06}$ | 0.023 | Calculated via REFPROP [17] at $T$ and $P$ of measurement |
| **Pressure expansion coefficient for the cylinder, $\varepsilon_{eff}$ [1/kPa]** | $5.2\text{x}10^{-09}$ | 20 | $-1.4\text{x}10^{-07}$ | < 0.001 | Reference [10] |
| **Pressure expansion coefficient for the connecting volume, $\varepsilon_{cv}$ [1/kPa]** | $5.2\text{x}10^{-09}$ | 20 | $-3.3\text{x}10^{-08}$ | < 0.001 | Reference [10] |
| **Combined Standard Unc. ($k$ = 1) [%] =** | **0.013** | | | | |

Table 7. Uncertainty budget for volumetric flow at the MUT for the 2.5 L/s LFS corresponding to Equation (9b).

| **Vol. Flow; $Q_{MUT}$ [L/s]**<br><br>**$Q_{MUT}$ = 0.06 [L/s]**<br><br>**Uncertainty Category** | **Nom. Value** | **Rel. Unc. ($k$ = 1) [%]** | **Norm. Sen. Coeff. ($S_c$) [-]** | **Contribution [%]** | **Comments** |
|---|---|---|---|---|---|
| **Volumetric prover $K$-factor, $K_v$ [cm$^3$/pulse]** | 0.35445 | 0.012 | 1 | 18.4 | From Water Draw |
| **Encoder pulses, $N_{en}$ [pulse]** | 2000 | 0.014 | 1 | 26.4 | Integer number of redundant pulses, one may be missed |
| **Duration of piston stroke, $\Delta t$ [s]** | 4 | 0.005 | -1 | 3.2 | Control charts for freq. cal. |
| **Linear thermal expansion coefficient of piston, cylinder, shafts, $\alpha_{st}$ [1/°C]** | $1.7\text{x}10^{-05}$ | 5 | $-1.7\text{x}10^{-05}$ | < 0.001 | See reference [9, 10] |
| **Linear thermal expansion coefficient of encoder material, $\alpha_{en}$ [1/°C]** | $8\text{x}10^{-06}$ | 5 | $-6.0\text{x}10^{-06}$ | < 0.001 | See reference [9, 10] |
| **Fixed connecting volume (not including unswept cylinder volume), $V_{cv}$ [cm$^3$]** | 260 | 10 | $-1.7\text{x}10^{-06}$ | < 0.001 | Calculated from LFS geometry measurements |
| **Linear thermal expansion coefficient of fixed connecting volume, $\alpha_{cv}$ [1/°C]** | $1.7\text{x}10^{-05}$ | 5 | $4.9\text{x}10^{-07}$ | < 0.001 | See reference [9, 10] |
| **Variable connecting volume (i.e., unswept cylinder volume), $V^f_{cyl}$ [cm$^3$]** | 12592 | 10 | $-2.1\text{x}10^{-05}$ | 0.005 | Calculated from LFS geometry measurements |
| **Encoder (and room) temperature, $T_{en}$ [°C]** | 20.25 | 0.15 | 0.0023 | 0.015 | Temperature cal records and data from LFS |
| **Initial liquid temperature in the cylinder, $T^i_{cyl}$ [°C]** | 20.52 | 0.017 | -0.86 | 27.4 | Temperature cal records and data from LFS |
| **Final liquid temperature in the cylinder, $T^f_{cyl}$ [°C]** | 20.53 | 0.017 | 0.82 | 24.5 | Temperature cal records and data from LFS |
| **Initial liquid pressure in the cylinder, $P^i_{cyl}$ [kPa]** | 527 | 0.06 | 0.0046 | 0.01 | Pressure cal records and data from LFS |
| **Final liquid pressure in the cylinder, $P^f_{cyl}$ [kPa]** | 530 | 0.06 | -0.0044 | 0.009 | Pressure cal records and data from LFS |

Continuation of Table 7.

| Uncertainty Category | Nom. Value | Rel. Unc. ($k$ = 1) [%] | Norm. Sen. Coeff. ($S_c$) [-] | Contribution [%] | Comments |
|---|---|---|---|---|---|
| **Initial liquid temperature in the fixed connecting volume, $T^{i}_{cv}$ [°C]** | 20.90 | 0.017 | -0.015 | 0.008 | Temperature cal records and data from LFS |
| **Final liquid temperature in the fixed connecting volume, $T^{f}_{cv}$ [°C]** | 20.87 | 0.017 | 0.015 | 0.008 | Temperature cal records and data from LFS |
| **Initial liquid pressure in the fixed connecting volume, $P^{i}_{cv}$ [kPa]** | 512 | 0.06 | $8.8\text{x}10^{-05}$ | < 0.001 | Pressure cal records and data from LFS |
| **Final liquid pressure in the fixed connecting volume, $P^{f}_{cv}$ [kPa]** | 514 | 0.06 | $-8.8\text{x}10^{-05}$ | < 0.001 | Pressure cal records and data from LFS |
| **Liquid temperature at the MUT, $T_{mut}$ [°C]** | 20.61 | 0.017 | 0.056 | 0.1 | Temperature cal records and data from LFS |
| **Liquid pressure at MUT, $P_{mut}$ [kPa]** | 520 | 0.06 | -0.00024 | < 0.001 | Pressure cal records and data from LFS |
| **Liquid volumetric thermal expansion coefficient, $\beta$ [1/°C]** | 0.00019 | 0.003 | $1.3\text{x}10^{-05}$ | < 0.001 | Derived from Temperature/density relationship determined by NIST. |
| **Liquid isothermal compressibility factor, $\kappa$ [1/kPa]** | $4.6\text{x}10^{-07}$ | 20 | $-2.2\text{x}10^{-05}$ | 0.024 | Calculated via REFPROP [17] at $T$ and $P$ of measurement |
| **Pressure expansion coefficient for the cylinder, $\varepsilon_{eff}$ [1/kPa]** | $5.2\text{x}10^{-09}$ | 20 | $3.9\text{x}10^{-06}$ | < 0.001 | Reference [10] |
| **Pressure expansion coefficient for the connecting volume, $\varepsilon_{cv}$ [1/kPa]** | $5.2\text{x}10^{-09}$ | 20 | $-7.6\text{x}10^{-09}$ | < 0.001 | Reference [10] |
| **Combined Standard Unc. ($k$ = 1) [%] =** | **0.028** | | | | |

### 5.4 Combined and Expanded Uncertainty of the Meter Factor

The uncertainties given in the prior section are for the average volumetric flow at the MUT. NIST normally uses the LFSs to calibrate pulse generating flow meters, e.g. turbine meters. For a turbine meter, calibration results are often presented using the dimensionless parameter Strouhal number *St*:

$$St = \frac{f}{Q}\left(\frac{\pi d_{\text{MUT}}^3}{4}\right). \tag{19}$$

Therefore, to determine the uncertainty of a meter factor for a pulse generating MUT, we determine the sensitivity coefficients for each component by partial differentiation of Equation (19). The uncertainty terms are then combined by the root-sum-squares method (RSS) to obtain the relative combined uncertainty, $u_c$, which in turn, is multiplied by a coverage factor ($k$) determined by the Welch-Satterthwaite method [3, Section G.4] to give the relative expanded uncertainty, $U_e = k\,u_c$ at a confidence level of approximately 95 %.

$$\frac{U_e(St)}{St} = k\left(\frac{u_C(St)}{St}\right) = k\sqrt{\left(s_f\frac{u(f)}{f}\right)^2 + \left(s_Q\frac{u(Q)}{Q}\right)^2 + u(R)^2_{\mathrm{BED}}} \tag{20}$$

The uncertainty components for a calibration include the relative standard uncertainty of the frequency measurements, $u(f)/f$, the relative standard uncertainty of the actual volumetric flow, $u(Q)/Q$, and the reproducibility of the MUT, $u(R)^2_{\mathrm{BED}}$.[m] For uncertainty claims presented here, the MUT is defined as the best existing device (BED) on the LFS [18]. Partial differentiation shows that the sensitivity coefficient for frequency ($S_f$) is 1.0 and the sensitivity coefficient for volumetric flow ($S_Q$) is -1.0. The relative standard uncertainty of the frequency measurements is less than 0.01 % and the relative standard uncertainty for volumetric flow is given in Table 6 and Table 7 for the 0.1 L/s and the 2.5 L/s LFS, respectively. To measure the flow meter reproducibility, the sample standard deviation of ten measurements at flow points that span the range of operation of each LFS were used. Ten measurements were chosen because that is the number of repeat measurements recommended to customers during a NIST calibration. The MUT for the 0.1 L/s LFS reproducibility evaluation was a ¼"-diameter Coriolis meter. To cover the flow range of the 2.5 L/s LFS, two meters were used. For flows below 0.33 L/s a ¼"-diameter Coriolis meter (the same as used for the 0.1 L/s LFS) was used and for flows above this a dual-rotor turbine meter of 1"-diameter was used. The flow meter reproducibility is within 0.015 % and 0.010 % for the 0.1 L/s and the 2.5 L/s LFS, respectively. Figure 12 shows a comparison of the Coriolis meter's calibration of both LFSs. The error bars are the $k = 2$ uncertainties for each LFS.

Taking into consideration each component of Equation (20) leads to a combined standard uncertainty of 0.022 % and 0.032 % for the 0.1 L/s and the 2.5 L/s LFS, respectively. The effective degrees of freedom ($\upsilon_{\mathrm{eff}}$) that determines the $k$ value that gives a 95 % confidence level was determined by the Welch-Satterthwaite Method [3]:

m Note that the uncertainty in flow meter diameter can be neglected as long as the same reference diameter is used.

$$v_{\text{eff}} = \frac{\left(\frac{u_C(St)}{St}\right)^4}{\frac{u(R)_{\text{BED}}^4}{10-1} + \frac{\left(s_Q \frac{u(Q)}{Q}\right)^4}{\infty} + \frac{\left(s_f \frac{u(f)}{f}\right)^4}{\infty}} \tag{21}$$

The effective degrees of freedom for the 0.1 L/s LFS is 42 and for the 2.5 L/s LFS is 978, which for a 95 % confidence level corresponds to $k$ values of 2.01 and 2.0, respectively. Therefore the expanded uncertainty for the 0.1 L/s LFS is 0.044 % and for the 2.5 L/s LFS is 0.063 %.

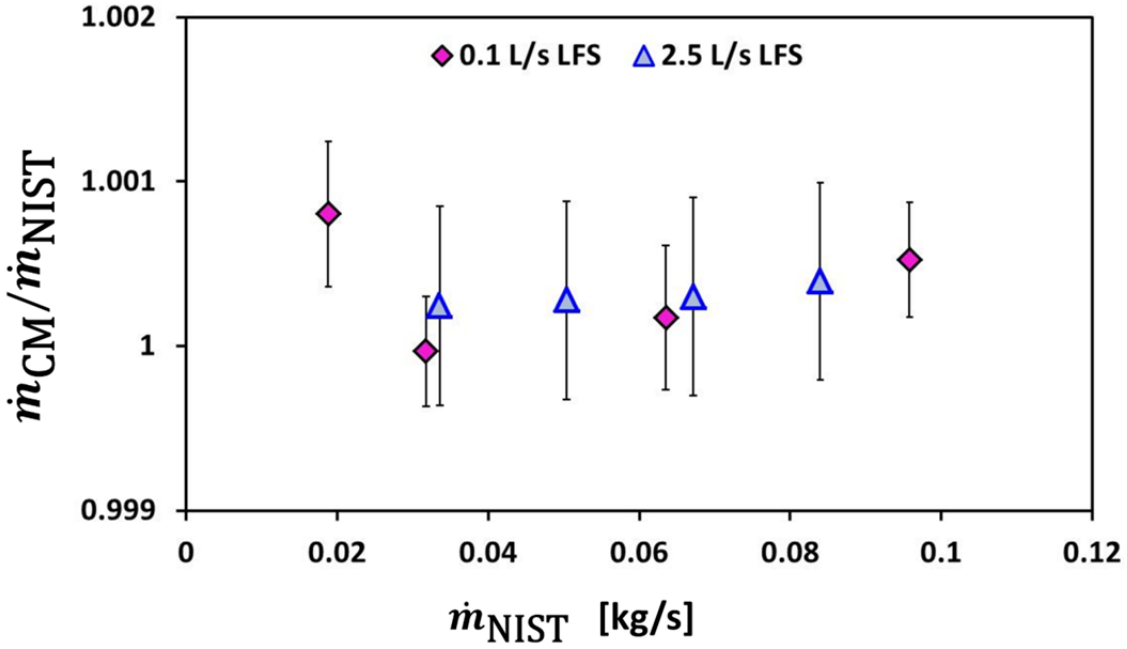


Figure 12. A comparison of the calibration of the Coriolis meter used as a "best existing device" for both LFSs.

## 6.0 Uncertainty of Meter Under Test

The uncertainty analysis reported above is for the 0.1 L/s and 2.5 L/s LFSs, including the associated connecting volumes and a repeatability component based on the most reproducible device or "check standard" available. The uncertainty analysis for a customer's MUT will depend on the flow meter type and the associated instruments used and therefore the

uncertainty claims for a customer's MUT may be larger than those reported here because the customer's MUT may not be as repeatable[n] or reproducible[o] as NIST's best existing device.

The uncertainties given in a NIST calibration report are for the calibration factor of the meter. When the flow meter is applied by the customer to measure flow, uncertainties beyond the NIST calibration must be considered. These uncertainty components include: installation effects, long term calibration changes, temperature effects on the meter, *etc*. The long term stability of the MUT is important as are reproducibility when turned-off and turned-on, and the day to day changes in its performance. These types of reproducibility errors can be an order of magnitude larger than the MUT's repeatability errors. The replicated uncertainty of the MUT is ascertained from multiple calibration results. By using this method, the total uncertainty of the calibration data for the test meter will include both contributions from the calibration system and MUT.

## 7.0 Summary

This document provides a description of the 2.5 L/s and 0.1 L/s liquid flow calibration standards operated by the National Institute of Standards and Technology (NIST) Fluid Metrology Group to provide flow meter calibrations for customers. The 0.1 L/s and 2.5 L/s flow standards measure flow by moving a piston of known cross-sectional area over a measured length during a measured time. The 0.1 L/s standard uses a passive piston prover technique where fluid is driven by a pump that in turn moves the piston. The 2.5 L/s standard uses a variable speed motor to move the piston and thereby move the fluid through the system. This facility is presently operated using a propylene glycol and water mixture that has kinematic viscosity of approximately 1.2 cSt at 21 °C but the ratio of propylene glycol to water can be altered to offer a different range of fluid properties. The 0.1 L/s standard has an uncertainty of ± 0.044 % over the flow range 0.003 L/s to 0.1 L/s (0.05 gal/min to 1.5 gal/min) and the 2.5 L/s standard has an uncertainty of ± 0.064 % over the flow range 0.02 L/s to 2.0 L/s (0.3 gal/min to 31 gal/min) (approximately 95 % confidence level uncertainties).

In this document, we provide an overview of the liquid flow calibration service and the procedures for customers to submit their flow meters to NIST for calibration. We derive the equation for calculating flow at the MUT, including the corrections for: 1) deviations from *reference conditions*, 2) *gradient effects* (*i.e.*, spatial non-uniformities in the temperature and/or pressure) and 3) *mass storage* effects (*i.e.* due to connecting volume between the cylinder and the MUT). In

n Repeatability is defined as the closeness of the agreement between the results of successive measurements of the same measurand carried out under the same conditions of measurement [1].

o Reproducibility is defined as the closeness of the agreement between the results of measurements of the same measurand carried out under changed conditions of measurement [1]

NIST's systems, the most significant correction terms are for deviations from reference conditions ($R_4$ and $R_5$) for the fluid temperature and pressure.

Finally we analyze the uncertainty of the flow standards, give supporting data, and provide a sample calibration report.

## 8.0 References


[1] International Vocabulary of Basic and General Terms in Metrology, 2nd ed. International Organization for Standardization. 1993; Geneva, Switzerland.

[2] Mattingly, G.E. Flow measurement proficiency testing. ISA Flow Measurement, 2nd ed. Practical Guides for Measurement and Control, Instrument Society of America. 2001; Ch. 28.

[3] Guide to the expression of uncertainty in measurement. International Organization for Standardization. 1993; Geneva, Switzerland.

[4] Yeh, T. T., Espina, P.I., Mattingly, G.E., and Briggs, N.R. An uncertainty analysis of a NIST hydrocarbon liquid flow calibration facility. Proceedings of HT/FED'04, HT-FED2004-56790, 2004 Heat Transfer/Fluids Engineering Summer Conference. 2004; Charlotte, NC.

[5] Pope, J.G., Wright, J. D., Johnson, A. N., and Moldover, M. R. Extended Lee model for the turbine meter and calibrations with surrogate fluids. Flow Measurement and Instrumentation. 2012; 24: 71 – 82.

[6] Pope, J.G., Wright, J. D., and Sheckels, S. D. Tests of the extended Lee model using three different turbine meters. Proceedings of the 8th International Symposium on Fluid Flow Measurement. 2012; Colorado Springs, CO.

[7] Wright, J. D., and Mattingly, G. E. NIST calibration services for gas flow meters: piston prover and bell prover gas flow facilities: NIST Special Publication SP 250-49, 1998.

[8] Manual of petroleum measurement standards: proving systems - small volume provers, 1st ed. American Petroleum Institute. 1993; Ch. 4.3.

[9] Lide, D. R. CRC Handbook of Chemistry and Physics. 73rd ed. Boca Raton, FL: CRC Press Inc.; 1992.

[10] Benson W., Harris, J., Stocker, H., Lutz, H. Handbook of Physics. New York, NY: Springer; 2006.

[11] Mattingly, G. E. The characterization of a piston displacement-type flow meter calibration facility and the calibration and use of pulsed output type flow meters. Journal of Research of the National Institute of Standards and Technology. 1992; Vol. 97, No. 5, Pg. 509.

[12] Aguilera, J. J., Yeh, T. T., and Wright, J. D. Inside diameter measurements for the cylinder of a 20 L piston prover. Proceedings of the 6th International Symposium on Fluid Flow Measurement. 2006; Queretaro Mexico.

[13] Taylor, B. N., and Kuyatt, C. E. Guidelines for the evaluating and expressing the uncertainty of NIST measurement results. 1994; NIST TN-1297.

[14] Coleman, H. W. and Steele, W. G. Experimentation and uncertainty analysis for engineers. 3rd ed. Ney York: John Wiley and Sons Inc.; 2009.

[15] Jaeger K. B., Davis R. S. A primer for mass metrology. NBS (U.S.) Special Publication SP 700-1, Industrial Measurement Series, 79 p. 5, 1984.

[16] Yeh, Tsyh T., Aguilera, Jesus J., Wright, John D. Hydrocarbon liquid calibration service: NIST Special Publication SP 250-1039, 2009.

[17] Lemmon, E. W., Huber, M. L., and McLinden, M. O. NIST reference fluid thermodynamic and transport properties – REFPROP. NIST Standard Reference Database 23, Version 9.0 User's Guide. U.S. Department of Commerce, Technology Administration, National Institute of Standards and Technology, Standard Reference Data Program. Gaithersburg, MD. November 2010.

[18] Calibration and Measurement Capabilities in the Context of the CIPM MRA, CIPM MRA-D-04 Version 2, September 2010, www.bipm.org/utils/common/CIPM_MRA/CIPM_MRA-D-04.pdf.

**Appendix A Sample Calibration Report**

# REPORT OF CALIBRATION

**FOR**

**A LIQUID FLOW METER**

**July 2, 2013**

Dual Rotor Turbine Flow Meter
Brand X, Model XX/XX
S/N: xxx

submitted by

Company X
666 Calibration Dr. West
Gaithersburg, MD 20899

(Reference: Purchase Order Number xxx, January 22, 2013)

NIST has two primary standards that are used to calibrate Liquid Flow meters: 1) The 0.1 Liter Per Second Liquid Flow Standard (0.1 L/s LFS); and 2) The 2.5 Liter Per Second Liquid Flow Standard (2.5 L/s LFS). The standards used in this calibration are traceable to the System International through national standards.

To cover the entire flow range, the meter under test was calibrated using both of the Liquid Flow Standards. The 0.1 L/s LFS was used for flows below 0.02 L/s (0.3 gallons/min) and the 2.5 L/s LFS was used for higher flows. To ensure consistency between the two standards the high flow data from the 0.1 L/s LFS (*i.e.*, flows between 0.02 L/s and 0.1 L/s) are included in the report.

The LFSs are piston provers that work on a volumetric principle. They determine the volumetric flow by displacing a known volume of liquid in a measured amount of time. During the calibration the output of the meter under test was gathered over the same time interval used by the primary standards to determine flow. The 95 % confidence level uncertainties of the 0.1 L/s LFS and the 2.5 L/s LFS are 0.044 % and 0.064 %, respectively.

Calibration results for the meter under test are presented in the tables and figures in this report in the form of Strouhal number, $St$, versus Roshko number, $Ro$.[p] The Strouhal number was calculated from the expression:

$$St = \frac{f\,\pi\,D^3}{4\dot{V}} \qquad (1)$$

where $f$ is the rotor frequency of the meter under test, $D$ is the diameter of the meter under test, and $\dot{V}$ is the actual volumetric flow at the meter under test. The Roshko number was calculated from the expression:

$$Ro = \frac{f\,D^2}{\nu} \qquad (2)$$

where $\nu$ is the liquid kinematic viscosity, obtained using the equations given below. The thermal expansion of the meter diameter was accounted for using the expression:

$$D = D_{20}\left[1 + \alpha(T - 20)\right] \qquad (3)$$

where, $D_{20}$ is the reference diameter of the meter under test at 20ºC (in this case, 1.25 cm or 0.5 in), $\alpha$ is the thermal expansion coefficient of the flow meter body material, taken to be $1.7\times10^{-5}$ /ºC, and $T$ is the fluid temperature in ºC.

Both of the NIST flow standards use a 5% by volume propylene glycol and water mixture. The fluid density and kinematic viscosity in each flow standard are calculated from temperature measurements using the following functions:

---

p Mattingly, G. E. The Characterization of a Piston Displacement Type Flow meter Calibration Facility and the Calibration and Use of Pulsed Output Type Flow meters. J. Res. Natl. Inst. Stand. Tech.: 1992; 97, pp. 509.

$$\rho = \rho_{21}\left[1-\beta\left(T-21\right)\right] \tag{4}$$

$$\nu = \left[\nu_0 + \nu_1\, T\right] \tag{5}$$

where, $\rho$ is the fluid density, in kg/m$^3$, $v$ is the kinematic viscosity, in centistokes, and $T$ is the fluid temperature in °C. These empirical correlations assume that the effect of pressure on the properties is negligible. The coefficients used in Equations 4 and 5 are listed in Table 1.

Table 1. Coefficients used to calculate the liquid properties of each flow standard.

| Flow Standard | $\rho_{21}$ [kg/m$^3$] | $\beta$ [1/°C] | $\nu_0$ [Centistokes] | $\nu_1$ [Centistokes/°C] |
|---|---|---|---|---|
| 0.1 L/s LFS | 1003.04 | 2.45E-04 | 1.8715 | -2.976E-02 |
| 2.5 L/s LFS | 1003.04 | 2.45E-04 | 1.8745 | -2.976E-02 |

The meter installation in both the 0.1 L/s LFS and the 2.5 L/s LFS are shown in Figure 1 and in Figure 2, respectively. As shown in the figures the same inlet and outlet tubes were used in both setups. Any extra pipe length upstream from the meter under test was of the same nominal diameter as the inlet tube.

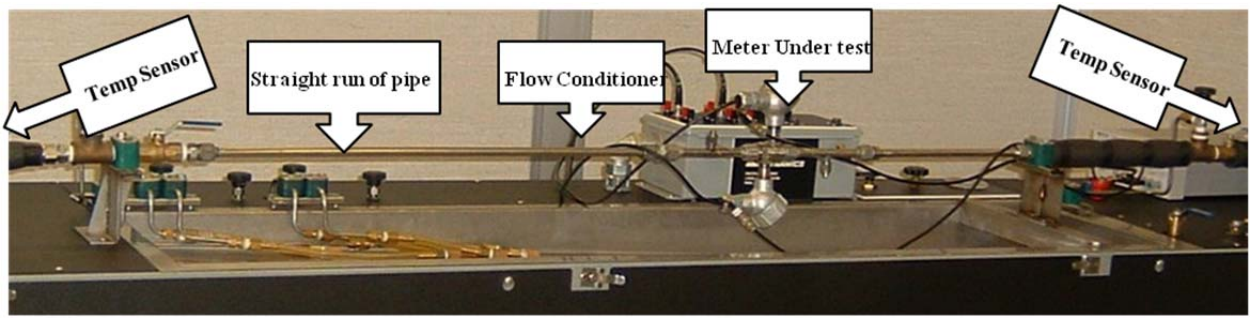


Figure 1. A photograph of the meter under test installed in the 0.1 L/s LFS

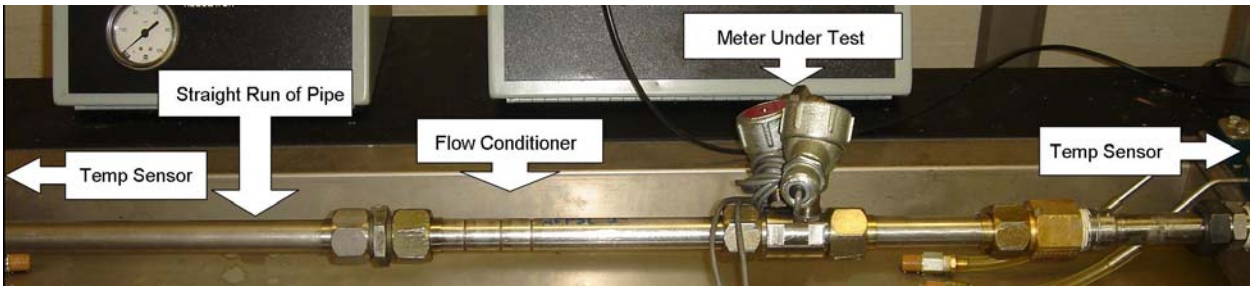


Figure 2. A photograph of the meter under test installed in the 2.5 L/s LFS.

An analysis was performed to assess the uncertainty of the calibration factors obtained for the meter under test.[q, r] This process involves identifying all of the significant uncertainty components and quantifying each of them at the 68 % confidence level. Additionally, we determine the sensitivity coefficients for each component by partial differentiation of Equation 1. The uncertainty terms are then combined by the root-sum-squares method (RSS) to obtain the relative combined uncertainty, $u_c$, which in turn, is multiplied by a coverage factor ($k \approx 2$) to give the relative expanded uncertainty, $U_e = k\,u_c$ at a confidence level of approximately 95 %.

$$\frac{U_e(St)}{St} = k \cdot \frac{u_c(St)}{St} = k \cdot \sqrt{\left(s_f \frac{u(f)}{f}\right)^2 + \left(s_{\dot{V}} \frac{u(\dot{V})}{\dot{V}}\right)^2 + u(R)^2} \qquad (6)$$

The uncertainty components for this calibration include the relative standard uncertainty of the frequency measurements, $u(f)/f$, the relative standard uncertainty of the actual volumetric flow, $u(\dot{V})/\dot{V}$, and the reproducibility of the meter under test, $u(R)$.[s] Partial differentiation shows that the sensitivity coefficient for frequency is $s_f = \frac{\partial St}{\partial f} \cdot \frac{f}{St}$ is 1.0 and the sensitivity coefficient for volumetric flow is $s_{\dot{V}} = \frac{\partial St}{\partial \dot{V}} \cdot \frac{\dot{V}}{St}$ is -1.0. The relative standard uncertainty of the frequency measurements is less than 0.01% while the relative standard uncertainty for volumetric flow is larger and depends on the flow standard used. For the 2.5 L/s LFS the expanded (95 % confidence level) volume flow uncertainty is 0.056 %[t] while for the 0.1 L/s LFS the standard volume flow uncertainty is 0.025 %.

---

q Taylor, B. N. and Kuyatt, C. E. Guidelines for Evaluating and Expressing the Uncertainty of NIST Measurement Results. NIST TN 1297; 1994 edition.

r Coleman, H. W. and Steele, W. G. Experimentation and Uncertainty Analysis for Engineers. New York: John Wiley and Sons; 1989.

s Note that the uncertainty in flow meter diameter can be neglected as long as the same reference diameter is used.

t For the 2.5 L/s LFS the relative expanded uncertainty for the volumetric flow at a meter under test is 0.06 % ($k = 2$) so that its relative standard uncertainty is 0.03 % ($k = 1$).

To measure the flow meter reproducibility, the standard deviation of 10 measurements was used to calculate the relative standard uncertainty (*i.e.*, the sample standard deviation divided by the average and expressed as a percentage) at each of the nominal flows. The flow meter reproducibility is a type A uncertainty, while all of the other uncertainty components are type B. Using the uncertainty values given above and Equation 6 yield the relative expanded uncertainties for the meter factors listed in the data tables and shown as error bars in the figures.

The calibration and uncertainties presented here are only valid over the range of the NIST calibration for this flow meter. When the flow meter is used at flows below the bearing dependent range[u] (typically 10 % of maximum[v]) additional uncertainties due to kinematic viscosity of the fluid being metered must be considered. These uncertainties arise from the use of the flow meter in a fluid of different kinematic viscosity than the fluid used during calibration and from the kinematic viscosity changing during use due to temperature changes. Turbine flow meters are insensitive to kinematic viscosity at flows above the bearing dependent range. The uncertainties given here are for the calibration factor of the meter. When the flow meter is applied by the customer to measure flow, uncertainties beyond the NIST calibration must be considered. These uncertainty components include: installation effects, long term calibration changes, temperature effects on the meter, etc.

---

u Pope JG, Wright JD, Johnson AN, Moldover MR. Extended Lee Model for the Turbine Meter and Calibrations with Surrogate Fluids. Flow Measurement and Instrumentation: 2012; 24: 71 – 82.

v 10 % of the maximum flow is a rough estimate of when kinematic viscosity effects turbine meter calibrations. The maximum flow at which kinematic viscosity introduces extra uncertainty is specific to a meter and can only be determined by calibration in a minimum of two fluids with different kinematic viscosities.

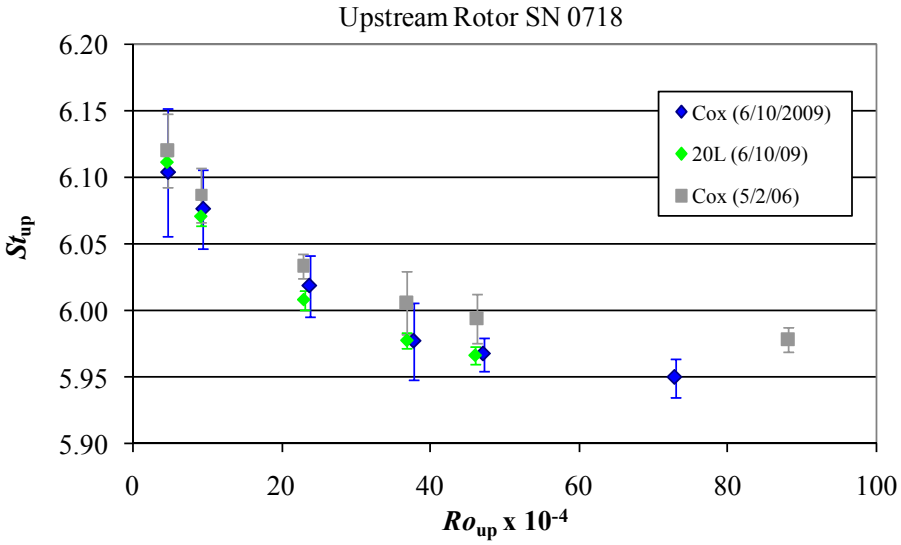


Figure 3. Calibration results for the upstream rotor of meter SN: xxx. (Older data shown for comparison purposes only. Note the 20-L is now the 2.5 L/s LFS and the COX benches have been de-commissioned). This figure is for illustration purposes only. To date, no turbine meter has been calibrated on both LFSs.

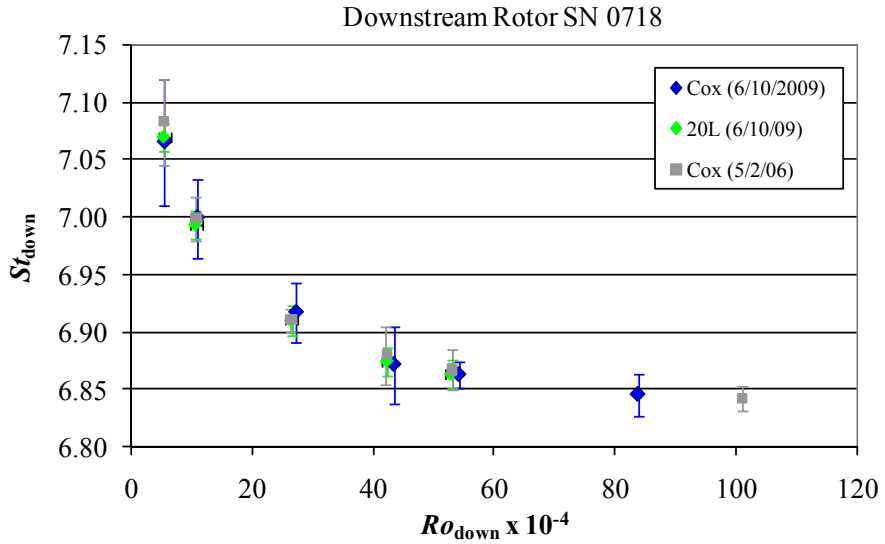


Figure 4. Calibration results for the downstream rotor of meter SN: xxx. (Older data shown for comparison purposes only. Note the 20-L is now the 2.5 L/s LFS and the COX benches have been de-commissioned). This figure is for illustration purposes only. To date, no turbine meter has been calibrated on both LFSs.

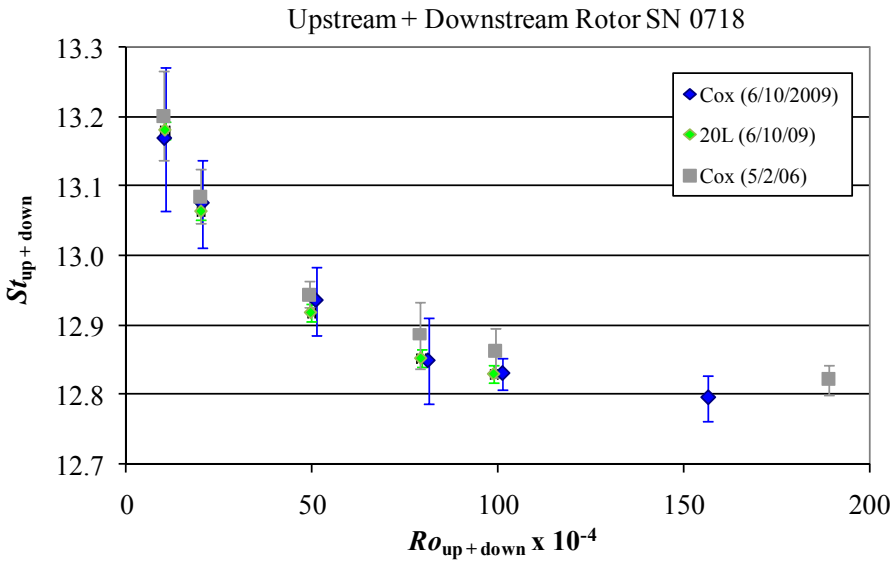


Figure 5. Calibration results for the upstream rotor plus the downstream rotor of meter SN: xxx where $St = St_{up} + St_{down}$ and $Ro = Ro_{up} + Ro_{down}$ .(Older data shown for comparison purposes only. Note the 20-L is now the 2.5 L/s LFS and the COX benches have been de-commissioned). This figure is for illustration purposes only. To date, no turbine meter has been calibrated on both LFSs.

## 2.5 L/s LFS DATA

Table 2. Tabulated results from the 2.5 L/s LFS for the upstream rotor of meter SN: xxx.

| $T_{liq}$ | $\rho$ | $\nu$ | $\dot{V}$ | $f$ | $Ro$ x $10^{-4}$ | $St$ | $U_{k=2}$ |
|---|---|---|---|---|---|---|---|
| [C] | [kg/m3] | [$m^2$/s] | [$cm^3$/s] | [1/s] | [-] | [-] | [%] |
| 22.32 | 1002.71 | 1.21E-6 | 27.654 | 27.506 | 1.47 | 12.803 | 0.26 |
| 22.36 | 1002.70 | 1.21E-6 | 62.877 | 65.352 | 3.50 | 13.378 | 0.09 |
| 22.38 | 1002.69 | 1.21E-6 | 83.011 | 86.756 | 4.64 | 13.452 | 0.10 |
| 22.40 | 1002.69 | 1.20E-6 | 110.681 | 115.845 | 6.20 | 13.472 | 0.11 |
| 22.40 | 1002.69 | 1.20E-6 | 138.339 | 144.454 | 7.74 | 13.440 | 0.07 |

Table 3. Tabulated results from 2.5 L/s LFS for the downstream rotor of meter SN: xxx.

| $T_{liq}$ | $\rho$ | $\nu$ | $\dot{V}$ | $f$ | $Ro$ x $10^{-4}$ | $St$ | $U_{k=2}$ |
|---|---|---|---|---|---|---|---|
| [C] | [kg/m3] | [$m^2$/s] | [$cm^3$/s] | [1/s] | [-] | [-] | [%] |
| 22.32 | 1002.71 | 1.21E-6 | 27.654 | 27.506 | 1.47 | 12.803 | 0.26 |
| 22.36 | 1002.70 | 1.21E-6 | 62.877 | 65.352 | 3.50 | 13.378 | 0.09 |
| 22.38 | 1002.69 | 1.21E-6 | 83.011 | 86.756 | 4.64 | 13.452 | 0.10 |
| 22.40 | 1002.69 | 1.20E-6 | 110.681 | 115.845 | 6.20 | 13.472 | 0.11 |
| 22.40 | 1002.69 | 1.20E-6 | 138.339 | 144.454 | 7.74 | 13.440 | 0.07 |

Table 4. Tabulated results from the 0.1 L/s LFS for the upstream rotor plus the downstream rotor of meter SN: xxx.

| $T_{liq}$ | $\rho$ | $\nu$ | $\dot{V}$ | $f$ | $Ro$ x $10^{-4}$ | $St$ | $U_{k=2}$ |
|---|---|---|---|---|---|---|---|
| [C] | [kg/m3] | [$m^2$/s] | [$cm^3$/s] | [1/s] | [-] | [-] | [%] |
| 22.32 | 1002.71 | 1.21E-6 | 27.654 | 27.506 | 1.47 | 12.803 | 0.26 |
| 22.36 | 1002.70 | 1.21E-6 | 62.877 | 65.352 | 3.50 | 13.378 | 0.09 |
| 22.38 | 1002.69 | 1.21E-6 | 83.011 | 86.756 | 4.64 | 13.452 | 0.10 |
| 22.40 | 1002.69 | 1.20E-6 | 110.681 | 115.845 | 6.20 | 13.472 | 0.11 |
| 22.40 | 1002.69 | 1.20E-6 | 138.339 | 144.454 | 7.74 | 13.440 | 0.07 |

**0.1 L/s LFS DATA**

Table 5. Tabulated results from the 0.1 L/s LFS for the upstream rotor of meter SN: xxx.

| $T_{liq}$ | $\rho$ | $\nu$ | $\dot{V}$ | $f$ | $Ro$ x $10^{-4}$ | $St$ | $U_{k=2}$ |
|---|---|---|---|---|---|---|---|
| [C] | [kg/m3] | [$m^2$/s] | [$cm^3$/s] | [1/s] | [-] | [-] | [%] |
| 22.32 | 1002.71 | 1.21E-6 | 27.654 | 27.506 | 1.47 | 12.803 | 0.26 |
| 22.36 | 1002.70 | 1.21E-6 | 62.877 | 65.352 | 3.50 | 13.378 | 0.09 |
| 22.38 | 1002.69 | 1.21E-6 | 83.011 | 86.756 | 4.64 | 13.452 | 0.10 |
| 22.40 | 1002.69 | 1.20E-6 | 110.681 | 115.845 | 6.20 | 13.472 | 0.11 |
| 22.40 | 1002.69 | 1.20E-6 | 138.339 | 144.454 | 7.74 | 13.440 | 0.07 |

Table 6. Tabulated results from the 0.1 L/s LFS for the downstream rotor of meter SN: xxx.

| $T_{liq}$ | $\rho$ | $\nu$ | $\dot{V}$ | $f$ | $Ro$ x $10^{-4}$ | $St$ | $U_{k=2}$ |
|---|---|---|---|---|---|---|---|
| [C] | [kg/m3] | [$m^2$/s] | [$cm^3$/s] | [1/s] | [-] | [-] | [%] |
| 22.32 | 1002.71 | 1.21E-6 | 27.654 | 27.506 | 1.47 | 12.803 | 0.26 |
| 22.36 | 1002.70 | 1.21E-6 | 62.877 | 65.352 | 3.50 | 13.378 | 0.09 |
| 22.38 | 1002.69 | 1.21E-6 | 83.011 | 86.756 | 4.64 | 13.452 | 0.10 |
| 22.40 | 1002.69 | 1.20E-6 | 110.681 | 115.845 | 6.20 | 13.472 | 0.11 |
| 22.40 | 1002.69 | 1.20E-6 | 138.339 | 144.454 | 7.74 | 13.440 | 0.07 |

Table 7. Tabulated results from the 0.1 L/s LFS for the upstream rotor plus the downstream rotor of meter SN: xxx.

| $T_{liq}$ | $\rho$ | $\nu$ | $\dot{V}$ | $f$ | $Ro$ x $10^{-4}$ | $St$ | $U_{k=2}$ |
|---|---|---|---|---|---|---|---|
| [C] | [kg/m3] | [$m^2$/s] | [$cm^3$/s] | [1/s] | [-] | [-] | [%] |
| 22.32 | 1002.71 | 1.21E-6 | 27.654 | 27.506 | 1.47 | 12.803 | 0.26 |
| 22.36 | 1002.70 | 1.21E-6 | 62.877 | 65.352 | 3.50 | 13.378 | 0.09 |
| 22.38 | 1002.69 | 1.21E-6 | 83.011 | 86.756 | 4.64 | 13.452 | 0.10 |
| 22.40 | 1002.69 | 1.20E-6 | 110.681 | 115.845 | 6.20 | 13.472 | 0.11 |
| 22.40 | 1002.69 | 1.20E-6 | 138.339 | 144.454 | 7.74 | 13.440 | 0.07 |

For the Director of the National Institute of Standards and Technology,

Dr. Jodie G Pope
Mechanical Engineer,
Fluid Metrology Group
Sensor Science Division

Sherry Sheckels
Calibration Technician,
Fluid Metrology Group
Sensor Science Division

Physical Measurement Laboratory
National Institute of Standards and Technology